
# BRNO UNIVERSITY OF TECHNOLOGY

VYSOKÉ UČENÍ TECHNICKÉ V BRNĚ

## CENTRAL EUROPEAN INSTITUTE OF TECHNOLOGY BUT

STŘEDOEVROPSKÝ TECHNOLOGICKÝ INSTITUT VUT


# NEW TECHNIQUE ON A CHIP FOR RAPID DETECTION OF BIOLOGICAL MATERIALS

NOVÉ METODY PRO RYCHLOU DETEKCI BIOLOGICKÉHO MATERIÁLU NA ČIPU

**DOCTORAL THESIS**
DIZERTAČNÍ PRÁCE


**AUTHOR** — **Jelena Pejovič Simeunovič**
AUTOR PRÁCE

**SUPERVISOR** — **doc. Ing. Jaromír Hubálek, Ph.D.**
ŠKOLITEL



**BRNO 2020**

## ABSTRACT

This work proposes a technique for on-chip separation and detection of quantum dots (QDs) conjugated with various proteins in order to study the influence of the coupling agent on a quenching of QD fluorescence intensity caused by conjugation to a protein and to perform multi-analyte immunoassay to identify small amounts of the protein. Under optimal conditions, bioconjugated QDs were successfully separated from free QDs within 10 minutes. Particles and target solutions were mixed, and on-chip detection was performed using a device developed in our laboratory. Only one excitation light source was used in combination with several filters for different emission wavelengths. Fluorescence emitted by the two types of conjugated QDs could then be recorded simultaneously since the QDs emitted light at different wavelengths while being excited at the same wavelength. By mixing two types of QDs bioconjugated with two kinds of proteins and antibodies we were able to detect immunocomplex peaks with varying areas. The peak area depended on concentration of QDs and antigens, on the progress of antibody-antigen reaction and proved to be linearly correlated with the antigen concentration. We showed that on-chip capillary electrophoresis of QDs can be used as a sensitive technique for detection of biological molecules. The main benefits of this method are simplicity, small sample and reagent volume requirements, and high efficiency of separation.



## ABSTRAKT

Tato práce navrhuje techniku separace a detekce na čipu pro kvantové tečky (QD, „quantum dots“) konjugované s různými proteiny, za účelem sledování vlivu vazebného činidla na potlačení intenzity fluorescence QD způsobené konjugací s proteinem a za účelem provedení multianalytické imunoanalýzy k identifikaci malých množství daného proteinu. Za optimálních podmínek byly biokonjugované QD úspěšně odděleny od těch nezkonjugovaných během 10 minut. Částice a cílové roztoky byly smíchány a detekce na čipu byla provedena za pomoci zařízení vyvinutého v naší laboratoři. Byl použit pouze jeden zdroj excitačního světla v kombinaci s několika filtry pro různé emisní vlnové délky. Fluorescence emitovaná dvěma typy konjugovaných QD mohla být poté zaznamenána současně, protože QD emitovaly světlo na různých vlnových délkách, ačkoliv byly excitovány při stejné vlnové délce. Smícháním dvou typů QD biokonjugovaných se dvěma druhy proteinů a protilátek jsme dokázali detekovat imunokomplexní píky s různými plochami. Plocha pod píkem závisela na koncentraci QD a antigenů, na postupu reakcí protilátka–antigen a ukázalo se, že je lineárně korelována s koncentrací antigenu. Ukázali jsme, že kapilární elektroforéza QD na čipu může být použita jako citlivá technika pro detekci biologických molekul. Hlavními výhodami této metody jsou jednoduchost, malé požadavky na objem vzorku i činidla a také vysoká účinnost separace.



**KEY WORDS:** quantum dots, bioconjugation, capillary electrophoresis, immunoassays, fluorescence quenching

**KLÍČOVÁ SLOVA:** kvantové tečky, biokonjugace, kapilární elektroforéza, imunoanalytické systémy, zhášení fluorescence

## BIBLIOGRAPHIC CITATION:

PEJOVIČ SIMEUNOVIČ, Jelena. New technique on a chip for rapid detection of biological materials. Brno, 2020. Dostupné také z: https://www.vutbr.cz/studenti/zav-prace/detail/125713. Doctoral Thesis. Vysoké učení technické v Brně, Středoevropský technologický institut VUT, Central European Institute of Technology BUT. Supervisor Jaromír Hubálek.

# DECLARATION

I certify that the work presented in this thesis was performed independently, under the supervision of doc.Ing. Jaromír Hubálek Ph.D., and is original with the sole exception of the technical literature and other sources of information that are acknowledged in the text and reference list, and that the material has not been submitted, in whole or in part, for a degree at this or any other university.

Brno . . . . . .  . . . . . .

(author's signature)

# ACKNOWLEDGEMENTS

I would like to thank to my supervisor doc. Ing. Jaromír Hubálek, Ph.D. for accepting me in the group and for his valuable advices, technical and pedagogical support and patient during my studies. Also, I would like to thank to all my colleagues (past and present) from the group Smart Nanodevice at CEITEC VUT for their cooperation, professionalisms, lessons and suggestions not only academic but also from day-to-day life. Special gratitude goes to prof. Ing. Pavel Neužil, Dr., DSc. for his innovative ideas, discussions and technical advices.

My thesis is a result of several collaborations. I was fortune enough to spend eight months in Department of Nanobiotechnology at University of Natural Resources and Life Sciences in Vienna. Special gratitude goes to Univ. Prof. Dr. Erik Reimhult for his enthusiasm in research and optimism when facing dilemma. Big piece of collaborative effort was the work on a chip electrophoresis immunoassay for multiple antibodies which was done with professor Mirek Macka from School of Natural Sciences and Australian Centre for Research on Separation Science (ACROSS), University of Tasmania, whom I thank for his energy, clear vision and great knowledge that he was willing to share, and doc. Mgr. Markéta Vaculovičová, Ph.D., form Department of Chemistry and Biochemistry, Mendel University in Brno, whom I thank for being extremely generous with sharing her knowledge, lab equipment, and experimental materials.

My sincere gratitude goes to my family and friends. My friends for being there whenever I need them the most and for enjoyable distractions of my studies. My brother and mother for their support and encouragement and my husband for his love, trust and patient. Last, but not least I dedicate this work to Vuk and Lazar my biggest inspiration.

# TABLE OF CONTENTS

# 1. INTRODUCTION

The aim of this PhD thesis is to develop and test chip-based technique, for separation and detection of different biological material. The work presented in this thesis is concentrate on using lab on a chip (LOC) technology to detect and separate quantum dots (QDs) and bioconjugated QDs using capillary electrophoresis (CE) on a chip, as well as screen and detect multiple analytes with minimal sample processing and handling using CE immunoassay.

Due to development in medicine, chemistry, drug discovery, environmental industry, and other industries world has become very dependent on a (bio) chemical analysis. To preform chemical analysis in traditional way we need to have certain amount of sample (water, blood…), modern equipment in laboratories and skilled people to perform demanding procedures. All this steps are time, energy and money consuming. New trend in technology moves towards performing few laboratory functions on one device, so called LOC technology.

Performing analysis with this technology is much easier and available to individuals with no special training and skills. Aim of this technology is to make small, portable device, easy to use. This goal equipment should be smaller, portable, easier to operate and reliable. LOC technology represent all this steps required for an analysis on a miniaturized system.

One of the most important components of the LOC device is the chip in which sample of micro- and nanoliters and reagents are moved around with very high accuracy. By dramatically reducing amount of samples and regents used, LOC offers a significant decrease in the cost. Since LOC technology is closely related and overlap with microfluidics, part of physics that examines properties of fluid in micro and nano-scale, it is important to understand behavior of fluid in microscale to be able to fabricate functionalized device used in different application.

Quantum dots (QDs) are nanoparticles (NPs) composed of periodic groups of III–V or II–VI semiconductor materials such as ZnS, ZnSe, CdS, CdSe, CdTe, and others [1] . Their unique optical and electronic properties placed them between those of bulk materials and isolated molecules of atoms [2]. Due to their remarkable properties, such as high quantum yield, large Stokes shift, broad absorption spectra, long fluorescent lifetimes, size-tunable photoluminescent emissions, and low levels of photobleaching, QDs are very attractive candidates for use in biolabeling, biological assay, and imaging [3]. However, the core of QDs created with heavy metals such as cadmium and lead are toxic for living systems and cells. To address these issues, numerous studies have centered on the development of QDs composed of materials with reduced toxicity, such as carbon (including graphene-like), silicon, and I–III–IV semiconductors ($Ag_2S$, $Ag_2Te$) and others [4]. To enhance QDs solubility under physiological condition and reduce their toxicity, a lot of research has also been addressed to surface coating of QDs [5]. Even, these modified QDs bring doubts [6], and more research needs to be done to investigate QDs and their bioconjugation.

QDs were conjugated to proteins [7-9], antibodies [10-12], enzymes [13], DNA [14], and peptides [15] to could be used in wide range of biological application [16]. There are mainly two strategies to conjugate QDs to a biomolecule: electrostatic interaction and covalent conjugation. Conjugation based on electrostatic interaction is easier to operate but not stable, while covalent conjugation uses coupling agents which by modification of QD surface makes very stable complex [17]. So-called zero-length-cross-linking agents are mostly used as coupling agents, such as carbonyldiimidazole (CDI), 1-ethyl-3-(3-dimethylaminopropyl)carbodiimide (EDC), or two-step procedure combining EDC with N-hydroxysulfosuccinimide (sulfo-NHS), that conjugate carboxyl groups and amines to form stable covalent amide linkages [18].

CE has emerged as a powerful tool for separation and characterizing of mixtures used for instance in HPLC technique. In recent 10 years, separating QDs and other NPs [19, 20] is under the study and using in analytics is highly promising. On-a-chip electrophoresis has some advantages over the conventional one, since it requires low sample volume, fast separation time, and high separation efficiencies, and in addition, microchip platform provides the possibility to integrate sampling, separation, and detection on a chip [21].

Immunoassay is a type of a protein assay based on the immunoreaction between an antibody and antigen. High selectivity and strong nature of antibody-antigen interactions makes antibodies or related agents valuable as reagents for the measurement and detection of analytes in complex samples such as blood, plasma, serum, urine, tissue sample [22]. Most immunoassays are conventionally carried out using a microplate. However, bulk-scale assays often require long analysis times and large amounts of sample/reagents. Moreover, labor-intensive manipulations are required to mix the solutions for the immunoreaction, separate the free antibody from the antigen-antibody complex (bound/free (B/F) separation) for selective assays, with low background signals. In enzyme-linked immunosorbent assay (ELISA) [23], further sensitive detection can be achieved by using an enzyme-labeled secondary antibody and its substrate, but it needs a longer analysis time and complex procedures. To overcome these drawbacks, immunoassay methods based on microfluidic devices have been developed recently [24-26]. Many types of immunoassays involve some form of a separation step for examining either the various species that may contain a label or for separating the bound and non-bound forms of a labeled species form each other. CE as a separation component in immunoassays has been used widely [27, 28]. Microfluidic devices based on a CE offer several advantages such as rapid reactions due to a short length for diffusion, effective reactions due to high surface/volume ratio, and minimal consumption of samples and reagents. These microfluidic techniques enabled rapid immunoassays with minimal consumption of reagents and samples, although the difficulty in the fabrication of these devices remains a problem. Thus, the running costs of immunoassays have not been reduced markedly by the above-mentioned reported microfluidic assays. In our work we used Polydimethylsiloxane (PDMS) chip to perform on a chip CE proof concept immunoassay, to reduce the price of fabrication of a device.

The fluorescent immunoassays have gained popularity due to their sensitivity, diverse selection of fluorophores, easy operation and various readout modes [29]. Even though,

several multiplexed dye-based assays have been reported in literature [30, 31], their narrow absorption and broad tailed emission spectra caused problems, such as cross-signaling, poor emission and undesired loss of photoluminescence signal [32]. A variety of inorganic nanocrystals have been designed, synthesized, and functionalized, with the aim of utilizing their unique nanoscale properties to either improve existing biosensing methods or to develop new sensing strategies [33].

Detection of multiple biomarkers has recently received a great interest from biosensors community. The ability of multiplexed detection of biomolecules is the key in order to accelerate the advances in genomics, proteomics, and disease prevention. These diagnostic methods must be rapid, specific, sensitive and cost-effective.

Taking in consideration everything above and scientific importance for solving problems in bioconjugation of QDs and their separation and detection with on a chip platforms, aim of this thesis is on one side to investigate bonding between QDs and biomolecules and on the other side to detect multiple biomolecules using CE immunoassay.

We used a simple method to monitor the formation of protein–QD complex based on mobility changes. Detection and separation of BSA–QD conjugates were done in microfluidic system, with on-a-chip electrophoresis and optical detection. QDs and QD–protein conjugates were successfully separated using on-a-chip CE within 10 min. Conjugation of QDs with BSA was achieved via covalent coupling. FL-quenching efficiency and the aspect of quenching mechanism of QDs bounded with BSA were studied by FL spectroscopy. The results present that BSA can effectively quench FL of QDs, which could be explained by a covalent interaction between the NPs and the quencher (protein), demonstrating the formation of QD–BSA bioconjugates. The highest quenching effect was notable when EDC/sulfo-NHS is used as a crosslinker.

The following two proteins were selected for this study: bovine serum albumin (BSA) and mouse immunoglobulin G (mIgG). These model proteins were chosen with respect to the reliable, specific and selective immunoreactivity with appropriate antibodies exhibiting low cross-reactivity. Moreover, significantly different properties (molecular mass and pI) ensure optimal electrophoretic behavior for development and optimization of the method.

Developing of rapid, sensitive and reliable assay of bioanalytes is highly important in various industries including food, healthcare, pharmacy, etc. [1]. A method combining high selectivity of immunochemical reaction with the separation efficiency of CE was used to monitor the formation of QD-labeled immunocomplex based on electrophoretic mobility changes. Moreover the influence of antigen and QDs concentration on separation performance was studied. Using one excitation wavelength and two types of filter set up it was possible to detect two different immunocomplexes simultaneously.

Together, both QDs and CE on a chip can be applied as a sensitive technique for the detection of biological molecules. This method has the ability to screen and detect multiple analytes with minimal sample processing and handling.

The thesis is organized as follows. The Section 2 explains the basic concept of Lab on a Chip technology, microfluidics, capillary electrophoresis, immunoassay and usage of bioconjugated quantum dots in biotechnology and medicine. In the section 4 experimental

set up that was developed in our lab is presented as well as other experimental methods used. In the section 5 studying of quantum dot luminescence quenching effect caused by covalent conjugation with bovine serum albumin is presented. Section 6 explains multi-analyte immunoassay experiments based on quantum dots fluorescence using on a chip electrophoresis. Finally, the conclusions are summarized in Section 7.

# 2. STATE OF THE ART

## 2.1 Microfluidic systems and Lab on a chip technology

### 2.1.1 Lab on a chip technology- overview

Lab on a chip (LOC) technology scales down laboratory functions and processes to a miniaturized chip format. LOC technology has been attracting a lot of attention in the past few years in different fields, from engineering, biotechnology, chemistry, environmental engineering, agriculture and others. The increasing rate of publications in the different fields in this topic serves as evidence (Figure 1).

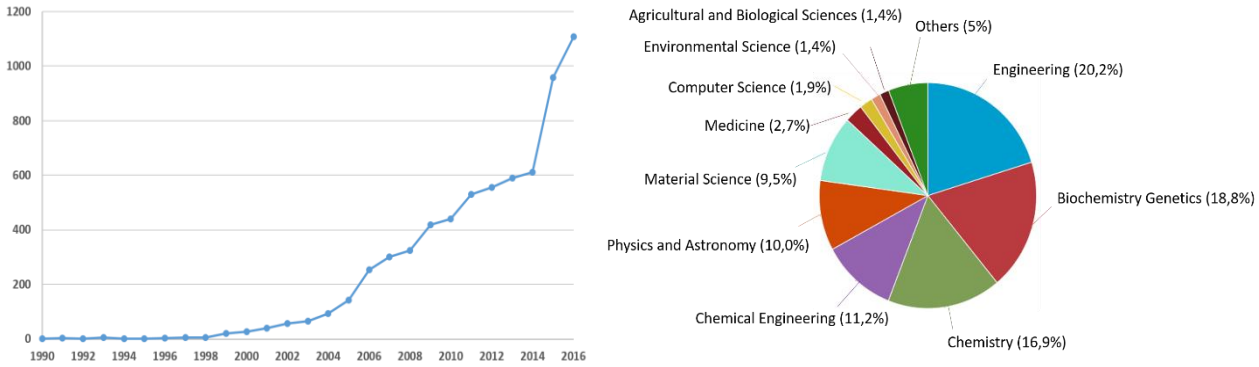


Figure 1 Number of publications and area of interest, in recent years regarding "Lab on a chip". Source: http://www.scopus.com

Characteristics of almost all LOC systems are several common features: microfluidics and sensing capabilities [34]. Microfluidics deals with fluid flow and flow control devices, and sensing capabilities includes different types of sensors.

In last two decades numbers of researches have stated a lot of advantages and disadvantages of using this technology. Main goal, if we talk about biological application, of this device is to be able to detect biological molecules, transport, mix and characterize them, all with one device.

For sure one of the biggest advantages is low consumption of fluid volume (sample, reagents, waste…) [35]. Reagents used in many biologic applications are rather expensive. When using pathogenic microorganisms usually it requires large cell numbers of a pure cell culture, involving time for pre-selection steps. When going from 50ml to 5nl that makes a huge impact. So making system that requires small volume of sample and reagent, makes a significant saving of money and time.

The other advantage is higher spatial resolution. Sensors in integrated circuit (IC) technology have small footprints, which increase spatial resolution. In fabrication of LOC devices new technologies such as complementary metal oxide semiconductor and other microtechnologies are used. One of the main characteristics of these technologies is high accuracy [36].

We can also achieve better process control by the automation of measurements in LOC devices by programing the controllers of the measurement, which also minimizes the manmade errors [37].

The massive parallelization due to compactness [38] as well as reproducibility of measurement are also some of advantages of using LOC devices. LOC devices are produced by using many sophisticated manufacturing process with good process control [39]. This makes this devices reproducible and chip-to-chip variation minimal. Faster analysis and response time due to faster reaction is also one of advantages of this technology.

Nevertheless microfluidic channels can approximate the size and flow conditions found in vivo capillaries [40]. Using of devices that can simulate size and elasticity as found in biology could lead to more accurate information and great understanding of physiology.

Many researchers believe that LOC may soon become important part of effort to improve quality of life within global health [41]. In countries where there are only few healthcare resources, one of the biggest problems is diagnostic of illness. Even when poor healthcare clinic have drugs to treat illness usually they have luck of diagnostic tools to identify patients that should receive the drugs. Idea is to solve this problem by creating microfluidic chips that will allow healthcare providers in poorly equipped clinics to perform diagnostic tests with no laboratory support. One of focuses of LOC research is diagnostic and manages of HIV infections [42]. Around 40 million of people are infected with HIV in the world today, yet only 1.3 million of these people receive antiretroviral treatment. Around 90% of people with HIV have never been tested for these diseases [43].

As a relatively new technology there are still some challenges to be overcome. Lab on-a-chip is a small scale industry and there are many effects that become dominate like capillary forces, surface roughness, and chemical interaction of materials used for fabrication on a reaction process. This sometimes of course makes process more complicated than in convectional laboratory equipment [44]. Detection principles may not always scale down in a positive way, leading to low signal-to-noise rations. Also, small channels make detection more demanding. They are more sensitive to adsorption of molecules on their surface, blocking of channels may occur as well as accumulation of bubbles.

Last few years a lot of research came up with solution to simplify an improving the manipulation of fluids on-chip. But there is still a lot of challenges to be overcome, especially in a field of microfluidics [11].

### 2.1.2 Microfluidics- definition and general overview

Microfluidics is the study that manipulate system with small amount of fluids ($10^{-9}$-$10^{-18}$ liters) using channels with dimension of hundreds micrometers to few nanometers [45]. It is a multidisciplinary field at the intersection of engineering, physics, chemistry, biochemistry, nanotechnology, and biotechnology, with practical applications in the design of systems in which low volumes of fluids are processed to achieve multiplexing, automation, and high-throughput screening [46].

One really obvious advantage of using microfluidics system is for sure small amount of fluid, faster time of analyses, separation and detection with high resolution and with lower costs. One less obvious characteristics of microfluidic system is behavior of fluids in those systems. Some of the factors like surface tension, energy dissipation, and fluidic resistance start to be dominated [47]. The flow in microfluidic channels can be characterized by Reynolds number (Equation 1), which compares the effect of the momentum of a fluid to the effect of viscosity:

$$Re = \frac{\rho v D}{\mu} \quad (1)$$

where $\rho$ is density of the fluid, $v$ is the mean velocity of the fluid, $D$ is the diameter of channel and $\mu$ is dynamic viscosity of fluid.

In microfluidic system, due to small dimension of channels, Reynolds number is usually much less than 100, often even less than 1 [48]. In this number regime, flow is completely laminar and no turbulence occurs. This offers fundamentally new capabilities in the control of concentrations of molecules in space and time. Together with new methods to fabricate chip, scientist were doing a lot of research trying to explain fundamental difference between the physics properties of fluids moving in large channels then those moving in small channels just few micrometer wide [46]. One of the most important properties of fluids in microfluidic system is that when two fluids stream together they do not mix, they flow in parallel, without turbulence, and mixing than occurs is the results of diffusion molecules across the interference between the fluids [49].

### 2.1.3 Fabrication of chip used in microfluidic systems

The chip in LOC devices is combination of integrated circuit (IC) and microfluidic systems. The IC parts are electronic circuit which control different functions, sensing, and actuation and detection parts. IC part can be mass produced using convectional IC technologies. IC industry expanded in last decades and lab-on-a chip is providing a lot of new avenues and opportunities for this industry. New markets can still be open. Also lab-on-a chip clearly profit for rapid development of IC technology and more accuracy on a low scale of devices fabricated using this technology. The microfluidic system can be fabricated

at low cost [50].

For example, Temiz et al. used a 20-way edge connector in order to interface a silicon chip to external electronic circuits used to generate and sense signals in cyclic voltammetry experiments Figure 2a [51] . Misiakos et al. developed a portable bioanalytical device for real-time protein and DNA detection [52]. They placed microfluidic chips having electrical contacts into reusable cartridges, inserted fluidic connections using a PDMS gasket, and plugged the assembled cartridge to an edge connector for electrical interfacing. More recently, Novo et al. developed an microfluidic immunoassay that utilizes autonomous capillary pressure for liquid flow and integrated photodiodes for optical detection, which are wire-bonded to a PCB and connected to the main device using an edge connector [53]. Similar electrical contacting principles are also used in commercial devices, such as hand-held glucometers working based on electrochemical sensing. Recently, Nie et al. fabricated paper-based analytical devices having printed electrodes and contact pads compatible with such commercial glucometers (Figure 2b) [54].

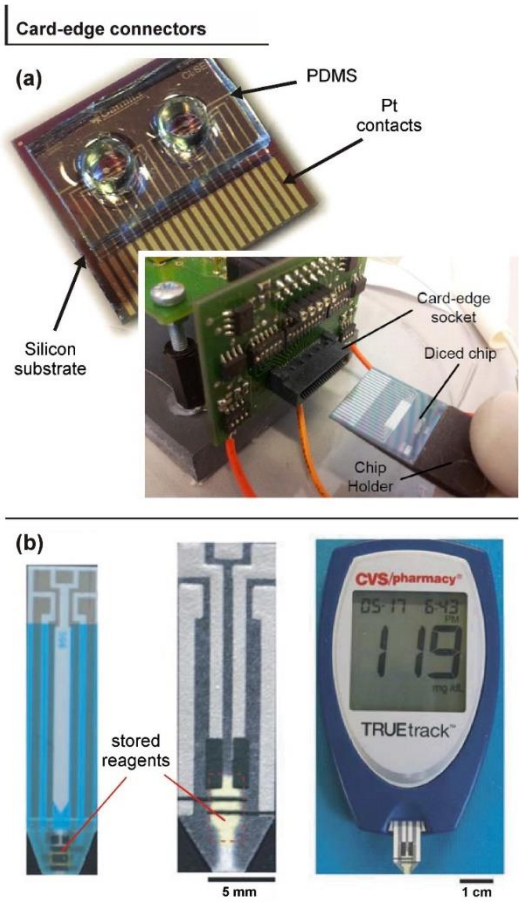


Figure 2 Edge connectors provide simple and non-permanent means for electrical connections for example to (a) driving electronics for cyclic voltammetric detection of analytes [51], [55] or (b) amperometric sensing of glucose and various compounds using a portable reader [54].

For fabrication of microfluidic chip in our experiments we used polydimethylsiloxane (PDMS), due to some disadvantages of other materials in this application. Silicon is rather expensive material but beside that is opaque in the visible/UV region [34]. This makes it unsuitable for system using optical detection like our system is. Glass is transparent, but it is amorphous and this makes it harder to etch than silicon.

### 2.1.4 PDMS based microfluidic systems

Polydimethylsiloxane called PDMS or dimethicone is a polymer widely used for the fabrication and prototyping of microfluidic chips. It is a mineral-organic polymer (a structure containing carbon and silicon) of the siloxane family (word derived from silicon, oxygen and alkane). Apart from microfluidics, it is used as a food additive (E900), in shampoos, and as an anti-foaming agent in beverages or in lubricating oils.

PDMS as a material for fabrication of a chip in microfluidic, has attracted a lot of attention due to its low cost and easy fabrication. While using a PDMS chip has some advantages, lot of research reported some disadvantages as well. Main advantages of using PDMS is low cost, easy to fabricate by replica modeling and flexible, which makes it promising in device fabrication, allowing easier integration of electrodes and ports of microdialysis coupling [56]. PDMS has been used for a fabrication of microfluidic chips that are used for biological aqueous solutions due it cures at low temperature, it is nontoxic and optically transparent down to 280 nm. List of advantages and disadvantages based on my recherché are listed in Table 1.

Table 1 List of advantages and disadvantages of using PDMS in fabrication of microfluidic devices

**PDMS**

| Advantages | Disadvantages |
|---|---|
| - Low cost<br>- Simple, rapid fabrication<br>- Ability to incorporate many electrode materials<br>- Easy integration of fluid connectors | - Short lifetime<br>- Adsorption of hydrophobic analytes<br>- Slow, irreproducible EOF in native PDMS:<br>• Migration time variability<br>• Difficult to electrokinetically manipulate fluid flow |

For the fabrication of microfluidic devices, PDMS (liquid) mixed with a cross-linking

agent is poured into a microstructured mold and heated to obtain an elastomeric replica of the mold (PDMS cross-linked).

PDMS empirical formula is $(C_2H_6OSi)n$ and its fragmented formula is $CH_3[Si(CH_3)_2O]nSi(CH_3)_3$, n being the number of monomers repetitions. Depending on the size of monomers chain, the non-cross-linked PDMS may be almost liquid (low n) or semi-solid (high n). The siloxane bonds result in a flexible polymer chain with a high level of viscoelasticity.

After "cross-linking" PDMS becomes a hydrophobic elastomer. Polar solvents, such as water, struggle to wet the PDMS (water beads and does not spread) and this leads to the adsorption of hydrophobic contaminants from water on PDMS surface. Surface treatment of PDMS is one of the most important thing to take inconsideration when using this material for fabrication of chip.

### 2.1.5 Microfluidics in analytic and bioanalytical what has been accomplished up to now

Microfluidics technology has a long history from basic research to diagnostic product used in hospital today. With the developing of gas chromatography, high-pressure liquid chromatography [26] and capillary electrophoresis [27] first research and development projects of manipulating liquid at high precision began. These techniques revolutionized chemical analysis because they allowed very small samples to be analysed with high sensitivity.

Meanwhile with the developing of continuous inject technology in the 1950s and the first commercial inject printers by Siemens the basics of precisely controlling fluids for printing began [57]. Inject printer were the first microfluidic devices. A high control on materials, interfaces, flow control and dimensionality gave the opportunity to achieve well performing devices. In 1975, Terry developed a silicon micromachined gas chromatograph [58].

The concept of miniaturized total chemical analysis was pioneered by Manz *et al.* [59] and resulted in development of microfluidic high-pressure liquid chromatography systems as well as microfluidic capillary electrophoresis in 1992 [60]. In the 2000s, additional microfluidic diagnostic devices were successfully commercialized. One successful product, the Biosite Triage ®[61] system provides a convincing implementation of microfluidics as an alternative to nitrocellulose membranes found in pregnancy tests. The chip has a sample metering area, hydrophobic valves to control incubation of the sample with a detection antibody, patterned receptor areas and a microfluidic channel that forms a loop around the main channel, wicking the sample through the device, and keeping the device small. There are more examples of successful microfluidic diagnostic products found on commercial websites and several specialized journals such as Lab on a Chip, Analytical Chemistry and

Clinical Chemistry, to name a few.

At present, microfluidics cover most, if not all, of the diagnostic segments with devices for pathogen detection, critical care, hematology, and blood typing. Microfluidics bring the possibility of using small volumes of samples that can be the basis for rapid tests done in a few minutes that are portable, and provide accurate diagnostics by carefully timing reactions involved in receptor/analyte bindings needed to carry out the test, and by designing accurate signals for a measuring device.

To date, microfluidic LOC devices have been incorporated in numerous types of biosensor assays [62], including microfluidic ELISA [63], on-chip PCR [64], particle immunoassays [65], and paper microfluidic assays [66]. Many of these developments have increased levels of specificity, sensitivity, ease-of-use, and portability.

## 2.2 On a chip electrophoresis

Electrophoresis is well known and powerful separation technique that has been very useful in the analysis of biological material.

On chip electrophoresis (microchip electrophoresis) has some advantages over conventional one since it requires low sample volume, fast separation time, high separation efficiencies [21], and additionally microchip platform provides the possibility to integrate sampling, separation, and detection on a chip.

Microchip electrophoresis was initially described by Harrison and Manz in 1992 [60]. The first high speed separation were published in 1994 by Ramey's group [67].

On chip electrophoresis is a liquid-phase separation method and analytes are separated based on differ in charge to hydrodynamic size ratio [68]. Typical electrophoresis on chip is done when channel of small dimension is filled with an electrolyte, followed by sample and a voltage is applied across channel. Analytes in channel are moved both due to electrophoretic mobility of analytes as well as the electroosmotic flow. In that way that small, high charged analytes moves faster. For CE separations, the velocity of a given analyte species is determinate by the mobility of the analyte plus the EOF as shown in Equation 2.

$$v = (\mu_e + \mu_{eof})E \qquad (2)$$

where *v* is the velocity of the analyte, $\mu_e$ is the electrophoretic mobility of the analyte, $\mu_{eof}$ is the EOF, and *E* is the electric field strength. Therefore, the electrooosmotc flow is a constant for a specific set of run conditions for all molecules being separated.

The electrophoretic mobility of analytes which is a function of analyte mass and net charge, is determinate using Equation 3 [69].

$$\mu_e = qE/6\pi\eta r \quad (3$$

where $q$ is the charge of the ionized analyte, $E$ is the applied electric field strength (v/cm), $\eta$ is the viscosity of the mobile phase, and $r$ is the radius of the molecule, which is related to its mass.

Because, the mass of a molecule is constant, the easiest way to influence electrophoretic separations is through changes in the mobile phase pH, which affect the charge on the molecules being separated.

### 2.2.1 Joule heating

Problems showed during performing on chip electrophoresis is Joule heating. Heat generated can cause a decrease in separation efficiencies, bubbling or boiling of fluid in channel and destroying of walls of channels.

Joule heating occurs due to electric current passing through the fluid in the channels generating heat. To get better separation efficiently with on chip electrophoresis, higher electric filed is applied [70]. High electric field is obtained using small channel lengths and high voltage which leads to accumulation of Joule heating [71]. General formula of Joule heating can be explained as Energy dissipated per unit time = Charge passing through resistor per unit time × Energy dissipated per charge passing through resistor. Assuming the element behaves as a perfect resistor and that the power is completely converted into heat, the formula can be re-written by substituting Ohm's law into the generalized power equation:

$$P = IV = I^2 * R = V^2/R \quad (4)$$

Where $P$ is the power (energy per unit time) converted from electrical energy to thermal energy, $I$ is the current travelling through the resistor or other element, $R$ is the resistance.

This internal heat generation is taken away not only by the coolant surrounding the capillary (through either air or liquid convection and radiation as well), but also by the cold liquid inside reservoirs connecting to the two ends of the capillary(through conduction) [72]. On neglecting the thermal end effects, Joule heating has been known to cause an increase and a radial gradient in the fluid temperature [73]. For this case, the profile of electroosmotic velocity remains plug-like in the bulk region despite the increased magnitude due to the drop of liquid viscosity [74]. However, both electrophoretic velocity and molecular diffusion of analyte species become non-uniform over the channel cross-section.

### 2.2.2 Electroosmotic flow

There is one more important characteristic of fluid flow in microfluidic systems. The driving force in electrophoresis is electroosmosis. Electroosmotic flow (EOF) is the liquid flow that originates when an ion-charged fluid is placed in a microchannel that has charges on its surface. As an example, the expanded region of the inner wall of a capillary (Figure 3), the ionized silanol groups (SiO) of the capillary wall attract cationic species from the buffer. Obviously, the buffer pH will determinate the fraction of the silanol groups that will be ionized. Understanding the amorphous nature of silica and the pKa range (4-6) associated with the various types of silanol groups is key. The layer formed closest to the surface of the channel is termed the "Inner Helmholtz" or "Stern" layer and is essentially fixed layer. Because the cations in the fixed layer only partially neutralize the negative charge on the capillary walls, the solution adjacent to the fixed layer contains more cations than anions and it is a diffuse layer called Outer Helmholtz Plane" (OHP). Together these two layers are known as the double layer.

Under an applied filed, cations in the OHP migrate in the direction of the cathode carrying waters of hydration with them. Because of the cohesive nature of the hydrogen bonding of the waters of hydration to the water molecules off the bulk solution, the entire buffer solution is pulled toward cathode. This EOF or "bulk flow" acts as a pumping mechanism to propel all molecules (cationic, neutral and anionic) toward the detector with separation ultimately being determinated by differences in the electrophoretic migration of the individual analytes.

Equation 5 describes the electroosmotic mobility in a capillary:

$$u_{eof} = \frac{\varepsilon\zeta}{4\pi\eta}. \tag{5}$$

The structure of the double layer defines the zeta potential, $\zeta$. The dielectric constant of the buffer filling the capillary is $\varepsilon$, and the viscosity of the solution near the capillary surface is $\eta$. All three of these terms contribute to the irreproducibility of EOF.

Advantage of EOF is that it is generated naturally during CE, and does not require external pumps or high-pressure interfaces. It can be generated and adjust simply through the applied potential.

If the EOF is low, diffusion of the analyte zones could result in substantial band broadening and, under conditions of very low EOF, some of the analytes may not reach the detector within a reasonable analysis time. Also, if EOF is very fast, components of the mixture may not have adequate "on-capillary time" for separation to occur [75].

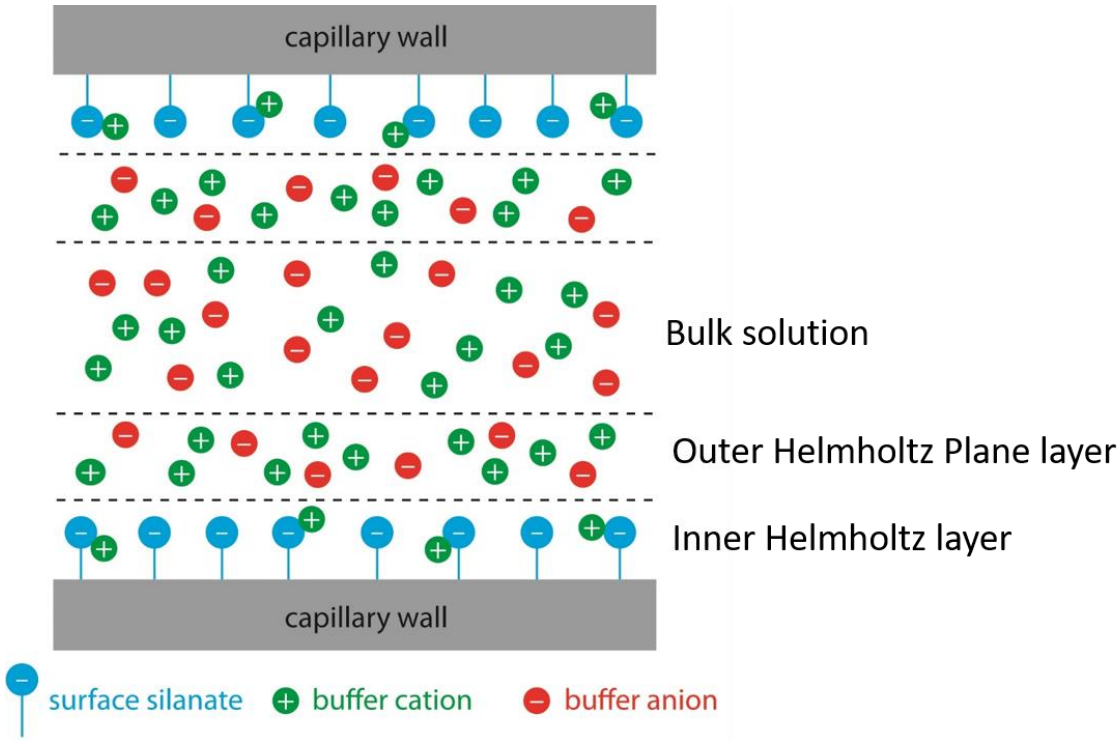


Figure 3 Electroosmotic flow in capillary

### 2.2.3 Buffers properties

Biological activity is significantly affected by groups of atoms in biological molecules becoming charged depending on pH. Changing the pH of a sample or adding chemical species to form a buffer can be needed for this reason.

Choosing right buffer for biological sample is useful for example to preserve native conformation of protein, to prevent aggregation of biomolecules, or to prevent adverse pH shift when samples partly evaporate or are diluted with liquid reagents on a chip. Intracellular fluid is an equilibrium between dihydrogen phosphate ions ($H_2PO_4$-) and hydrogen phosphate ions ($HO_4P_2$-). Phosphate buffered saline (PBS) is based on this chemistry and is one of the most common buffers used in biochemistry; it is also frequently used when a sample is spiked with known amounts of analyte of interest for calibrating or developing microfluidic devices.

Good *et al.* selected a variety of buffers based on criteria of ideal solutions for biochemical reactions [76]. Buffer compounds were selected according to criteria of value in biochemistry: a pKa between 6 and 8 where most biological reactions occur, maximal water solubility, cell membrane impermeability, minimal salt effects, soluble cation complexes, minimal optical absorbance of visible or ultraviolet light and ease of preparation.

A suitable background electrolyte (BGE) in capillary zone electrophoresis (CZE) must

meet some general requirements. Besides of the basic need of easy preparation, stability, good buffering and reproducible operation, it must also provide the necessary selectivity between the analytes separated. Bocek *et al*, did the research into the basic electromigration properties of BGEs based on phthalate that might have remained mostly unrecognized so far [77]. It is well known that the more components are present in the BGE used, the more complex is its electromigrational performance demonstrating itself especially in the generation of system peaks. Beside p*Ka* and molecular size, other factors to consider when choosing a buffer would include toxicity, solubility, UV absorption and the possibility of interaction with other species present in the solution.

Electrokinetic pumping can greatly simplify species transport in microfluidic systems, however Joule heating caused by the current flow through the buffer solution can lead to significant increases in the buffer temperature. The relatively low thermal conductivities associated with polymeric microfluidic substrates (such as PDMS) make the rejection of this heat more difficult [78].

## 2.3 Capillary electrophoresis immunoassay

Immunoassays have long been an important set of tools in clinical laboratories for the detection, diagnosis, and treatment of disease. Over the last two decades, there has been growing interest in utilizing CE as a means for conducting immunoassays with clinical samples. The resulting method is known as a CE immunoassay. This approach makes use of the selective and strong binding of antibodies for their targets, as is employed in a traditional immunoassay, and combines this with the speed, efficiency, and small sample requirements of CE.

### 2.3.1 Immunoassay

Immunoassays have been important tools in clinical chemistry for many decades [27]. In general, an immunoassay can be defined as a technique in which antibodies or antibody related substances are used as selective binding agents for chemical detection [27]. Antibodies are a group of glycoproteins that are produced by the immune system in response to a foreign agent, or antigen. The binding of an antibody with an antigen is a reversible process that occurs through noncovalent interactions. However, the fit of the antigen within an antibody's binding sites and the large variety of interactions that can occur allow this process to create a highly selective and strong complex that often has an association equilibrium constant in the range of $10^5$–$10^{12}$ $M^{-1}$ [79].

### 2.3.2 General formats for CE immunoassays

With the consideration of the nature of the analyte, labeling chemistry availability, the required assay sensitivity, dynamic range, and precision, the immunoassay methods can be classified in two basic forms: (I) heterogeneous immunoassays and (II) homogeneous immunoassays [80]. They are distinguished by the separation process. Homogeneous assays are accomplished by simply mixing the reagent samples, and heterogeneous assays are often carried out with washing and separation steps. The design of both forms can be further classified as competitive or non- competitive immunoassays. The competitive immunoassay relies on the competition between the antigen of interest and a constant amount of a similar but labeled antigen for a limited amount of specific antibody. The noncompetitive immunoassay uses an excess of labeled specific antibody toward the analyte of interest. The choices of which type of immunoassay is used, are based on the nature of the analyte, labeling chemistry availability, the required assay sensitivity, dynamic range, and precision.

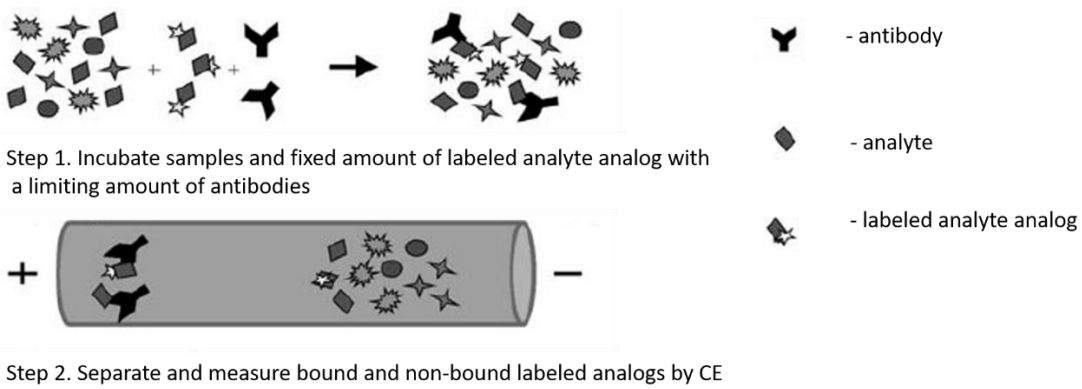


Figure 4 Scheme for a homogeneous competitive binding CE immunoassay, based on [81]

In this chapter we will more closely describe competitive binding format, since that format was used in our work. In this type of assay, all of the sample components and reagents are presented in the solution phase. Competition is created between the analyte and a labeled analog of the analyte (or “label”) by using a limited amount of antibodies, as is illustrated in Figure 4 [82]. After these components have been incubated and allowed to bind, CE is used to separate the free and antibody bound forms of the labeled analog. The amount of either the free or bound forms of the labeled analog is then measured and used as an indirect measure of the amount of analyte that was originally in the sample. This can be done because an increase in the amount of analyte will cause less of the labeled analog to bind to the antibodies, leading to an increase in the free form and a decrease in the bound form of the labeled analog.

### 2.3.3 Application of CE immunoassays

Immunoassays are central to research in the life sciences and clinical diagnostics [83]. They are routinely performed to detect disease markers and pathogens in patients as well as for therapy monitoring [84]. There are several features of immunoassays that make them appealing for use in clinical testing. For instance, the highly selective and strong nature of antibody–antigen interactions makes antibodies or related agents valuable as reagents for the measurement and detection of analytes in complex samples that include blood, plasma, serum, urine.

In many areas such as endocrinology, pharmaceutical measurements, protein and peptide analysis, immunology, infectious disease detection and oncology, CE immunoassay has been employed. In the field of endocrinology, these methods have been created to measure such analytes as insulin, glucagon, steroid hormones and others [85-87]. Pharmaceutical applications have included the use of CE immunoassyas for detecting drugs of abuse, therapeutic drug monitoring and measurement or study of potential toxic agents. In immunology CE immunoassay was used to monitor and profile agents such as interferons and interleukins, or in the detection of infectious agents like bacteria and prion proteins. Finally, various applications of CE immunoassays have been reported in the field of cancer, to detect cancer biomarkers, the assessment of DNA damage by potential carcinogens, and the determination of multi-drug resistance in cancer cells.

Portable devices for immunoassays are increasingly used in healthcare for decentralized and point-of-care testing [88], providing benefits of a shorter time to result and accessibility where there is limited infrastructure.

### 2.3.4 Gaps and opportunities in immunodiagnostics

A patient visit to a hospital typically follows these steps: (i) the patient is interviewed by the clinician who follows a differential diagnosis method and considers medical history, risk factors and the current problem, (ii) an examination is performed looking closely at critical aspects from the history and narrowing the list of possible causes, and (iii) tests are performed (such as blood tests and medical imaging) to further narrow the list and/or confirm the differential diagnosis. Immunodiagnostics are a critical part of the diagnosis process where the identification of key proteins helps to differentiate between major classes of disease: cardiovascular disease, pulmonary disease, infectious disease, metabolic disease (e.g. complications of diabetes mellitus) and cancer.

The way some diseases are treated has changed with the testing of certain analytes. A high level of cardiac markers (especially CK-MB, myoglobin and troponin I and T) can indicate an increased risk of heart disease [89] and are monitored routinely after a myocardial

infarction [90].Testing for the absence of D-dimer in circulating blood can exclude the presence of a pulmonary embolism [91]. Cancer can be diagnosed by detecting cancer markers using immunoassays on biopsy samples in conjunction with medical imaging. Cancer markers (such as prostate specific antigen (PSA) for prostate cancer and CA-125 for ovarian and colon cancer) are measured routinely to evaluate the progression of disease and the monitoring of therapy. It is important to note that although many new biomarkers are being discovered, biomarkers must be used within a medical context. The assessment of a clinician in combination with medical imaging and tests for panels of markers lead to a proper diagnosis. Diagnostics are essential for the identification and treatment of patients for pre-clinical and clinical research.

There is a pressing need for POC devices as perceived from biohazard threats, the aging population, the spread of infectious disease and the need for home testing and monitoring.

The way forward to developing such devices is sensed by looking at grand challenges and long unmet medical needs such as the rapid detection of infectious disease in resource poor settings, [42, 92] early diagnosis of disease via the detection of ultra-low concentration analytes and monitoring of therapy, especially during clinical trials of new drugs.

There are a variety of malaria POC devices available from different manufacturers all based in this case on an immunoassay test strip similar to a pregnancy test. Manufacturers have the same technology available to them: filter membranes, nitrocellulose membranes, spray deposition of high affinity detection and capture antibodies, labeling of antibodies using colloidal gold or latex particles, detection protocols and storage methods, yet a huge discrepancy arises in the performance and reproducibility of the different devices.

This evaluation of the performance of on the market POC devices illustrates the ubiquitous need for sensitive and accurate POC diagnostics, especially for infectious diseases. Ideally, they should also be reliable, low-cost, robust and easy to use. We think that microfluidic technology can lead to more accurate and reliable immunoassays than those performed using test strips owing to (1) a higher degree of control of the flow of liquids in microfluidics, (2) the possibility of miniaturizing test areas and thereby implementing controls and redundant detection regions, and (3) to the improvement of the assay conditions using specific microfluidic elements such as mixers and valves.

## 2.4 Quantum dots

Quantum dots (QDs) are nanoparticles composed of periodic groups of III-V or II-VI semiconductor materials such as ZnS, ZnSe, CdS, CdSe, CdTe, InP, and others [1]. Their unique optical and electronic properties placed them between those of bulk materials and isolated molecules of atoms [2]. In the past decades, quantum dots (QDs) have attracted much attention due their unique photochemical and photophysical properties [40].

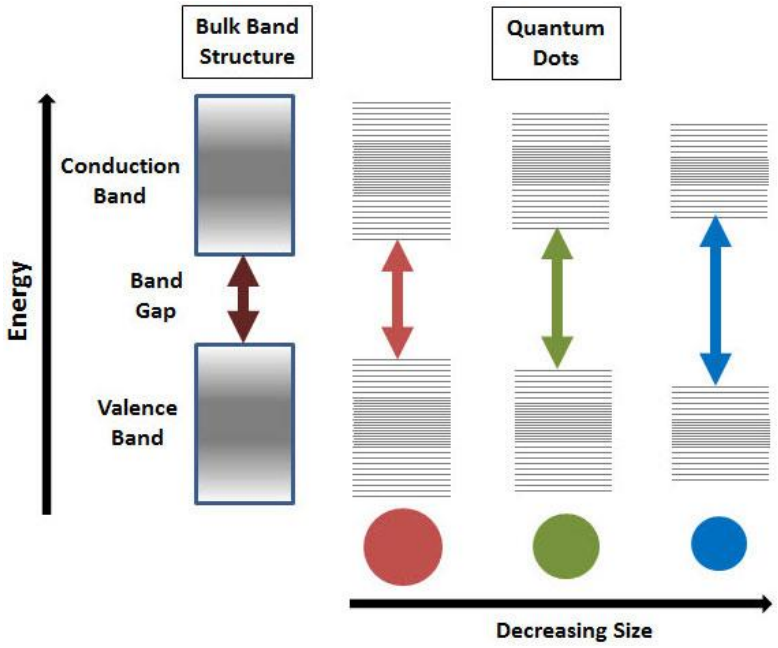


Figure 5 Schematic illustration of quantum confinement effect. Quantum confinement can shift the band gap of the semiconductor providing tunability dependent of the QDs. Similar to the „particle in a box" model, excitons in smaller nanocrystals experience stronger quantum confinement, resulting in larger photoluminescence energy or emission in shorter wavelengths (blue range).

Unique characteristics such as symmetric and narrow emission, continuous absorption spectra and high emission quantum yields originate from quantum confinement as well as their name quantum dots. The quantum confinement effects occur, when the nanoparticle radius is lower than one of these magnitudes: *ae*, *ah* and *aexc* (Bohr radius of electron, hole and exaction, respectively). The QDs fluorescent properties arise from the fact, that their excitation states/band gaps are spatially confined. In these small particles conductive and valence bands have been formed due to interaction of the highest occupied atomic levels of the atomic species and lowest unoccupied levels. Upon excitation an electron is promoted from the valence band to the conductive creating electrostatically bound electron-hole pair called exciton. In bulk materials electron and holes can move around but still remain together due to Coulomb electrostatic attraction, but in the crystal the exciton has a finite sized terminated by Bohr exciton diameter. If the particles size gets smaller than Bohr radius the exciton is spatially confined which results in increasing their energy causing energy level shifting to the higher levels. So it can be concluded that emission wavelength is dependent on the size photon's emission wavelength and can vary from UV to NIR wavelengths (400–1350 nm). Larger QDs having smaller band gaps emit red light, while smaller QDs emit blue light of higher energy [19]. These effects depend not only on the core size, but also on the chemical composition of the core (Figure 5).

### 2.4.1 Optical properties of QDs

QDs are relatively easy to prepare, biocompatible, stable and soluble in aqueous solutions.

Figure 6 shows the narrow emission and broad adsorption spectra of QDs, which makes them ideal candidate for multiple imaging. The broad absorption arise from the fact that in the single crystal QDs the absorption of a photon above the semiconductor band gap creates an electron hole pair that has increasing probability of occurrence as the energy of the photon is increased [93]. In the fact, QDs can be excited at any single wavelength below their characteristic absorbance to obtain varying emission by just changing the size of quantum dots. A very large Stoke's shift can also be observed that allows labelling of multiple biomolecules and cells under continuous illumination (Figure 6).

The emission spectra of QDs are narrow and symmetrical which makes it easy to distinguish one colour of QD from another colour of QD. The full width at half maximum (FWHM) of a single (CdSe)ZnS quantum dot's emission spectra could be as narrow as 13 nm at room temperature [94]. QDs' emission wavelength can be tuned from UV to near infrared by changing their composition and size (Figure 4). The shape of the QDs also has also an effect on the emission spectra. Hu *et al.* [95] discovered that quantum rods (elongated shape) showed linearly polarized emission, while spherical CdSe QDs' emission is circularly polarized or non-polarized [96, 97].

The radiative recombination of electrons and holes is also characterized by longer lifetime allowing QDs to demonstrate long fluorescence lifetimes as opposed to shorter lifetime of conventional fluorophores [98]. High resistance to photo bleaching is another desired property for designing fluorescence tags and QDs display exceptional stability against photo bleaching on continuous excitation [99, 100]. As compared to the organic fluorophores that bleach after only few minutes of exposure to the external radiation, QDs can cycle through repeated excitation and emission cycles for several hours.

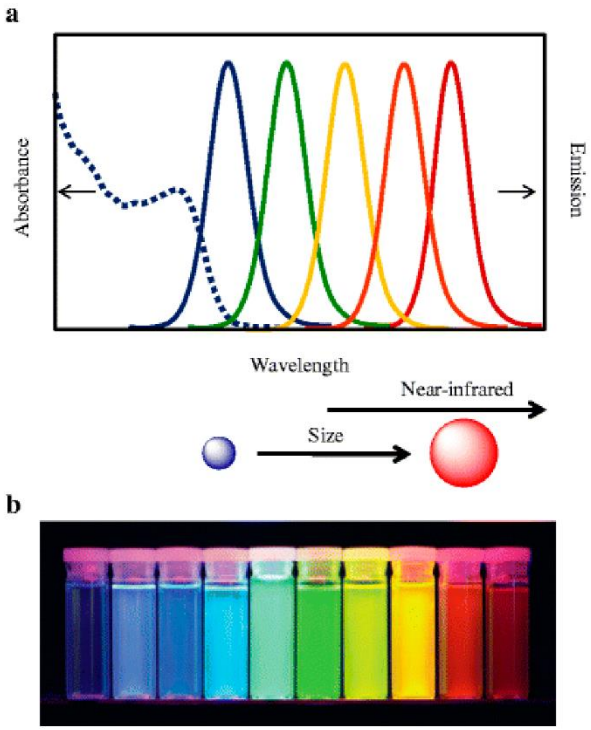


Figure 6 **a**: Size-tunable emission spectra of quantum dots (QDs); the dashed line exemplifies the absorption spectrum of the QD emitting at the lower wavelength. **b**: Size-tunable fluorescence properties of QDs: ten distinguishable emission colors of CdSe/ZnS QDs excited with a near-UV lamp. From left to right (blue to red), the emission maxima are located at 443, 473, 481, 500, 518, 543, 565, 587, 610, and 655 nm. (base on [28])

### 2.4.2 Fluorescence quenching

Quenching of fluorescence is a physicochemical process that decreases fluorescent intensity of light emitting molecules. We will focus our attention to two different ways of quenching: dynamic (collisional) and static (complex formation).

Dynamic quenching occurs when a random non-interactive collision of a small molecule deactivates the excited state of the fluorophore. Collisional quenching is observed with the collision of an excited state fluorophore and another molecule in solution (ions, oxygen, halogen, other fluorophores (self-quenching)), which can undergo electron transfer, spin-orbit coupling, and intersystem crossing to the excited triplet state without chemical alteration, resulting in deactivation of the fluorophore and return to the ground state [101].

Static one occurs when a small molecule makes a ground state complex with the fluorophore so that is becomes nonfluorescent. Here a complex of formation occurs between the fluorescing molecule at the ground state (F) and the quencher molecule (Q) through a strong coupling, such complex may not undergo excitation or, may be excited to

a little extent reducing the fluorescence intensity of the molecule (Figure 7) [102].

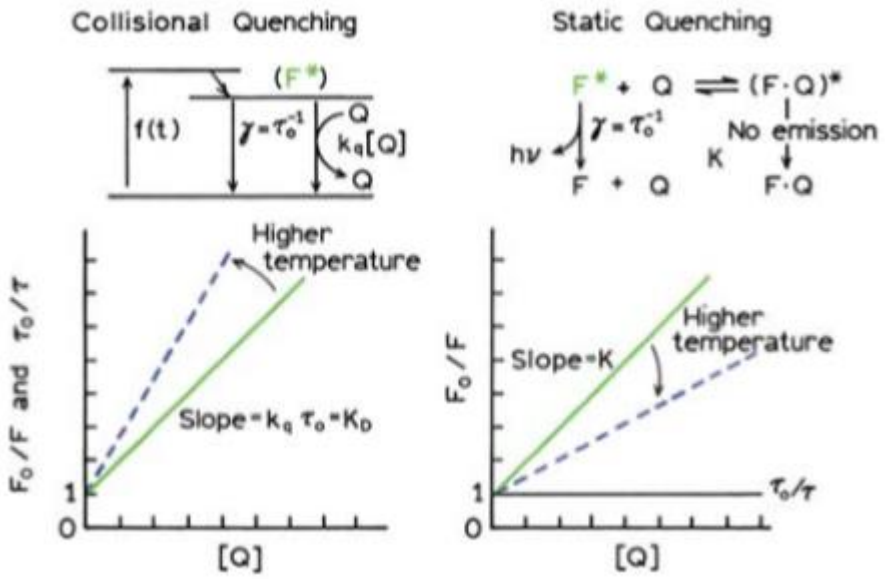


Figure 7 Comparison of dynamic and static quenching [101]

We can gain information about the fluorescence lifetime and excited state deactivation by introducing quenchers observing the fluorescence intensity as a function of their concentration. In the simplest case of quenching, the following relation, called the Stern-Volmer equation (Equation 6), holds:

$$\frac{I_0}{I} = 1 + K_{sv}\,[Q] \tag{6}$$

where $I_0$ and $I$ are the fluorescence intensities observed in the absence and presence, respectively, of quencher, [Q] is the quencher concentration and $K_{SV}$ is the Stern-Volmer quenching constant.

When the fluorophore can form a stable complex with another molecule, and if this ground-state is non-fluorescent then we say that the fluorophore has been statically quenched. In such case the dependence of the fluorescence as a function of the quencher concentration follows the relation (Equation 7):

$$\frac{I_0}{I} = 1 + K_a[Q] \tag{7}$$

where $K_a$ is the association constant of the complex.

In the case of static quenching the lifetime of the sample will not be reduced since those fluorophores which are not complex, and hence are able to emit after excitation, will have normal excited state properties [101]. The fluorescence of the sample is reduced since the quencher is essentially reducing the number of fluorophores which can emit.

If both static and dynamic quenching are occurring in the sample then the following

relation (8) holds:

$$\frac{I_0}{I} = \left(1 + k_q \tau_0 [Q]\right)(1 + K_a[Q]) \qquad (8)$$

Where $k_q$ is the bimolecular quenching constant and $\tau_0$ is the lifetime of the fluorophore in the absence of quencher.

In such a case then a plot of *Io/I* versus [Q] will have an upward curvature due to the $[Q]^2$ term (Figure 8).

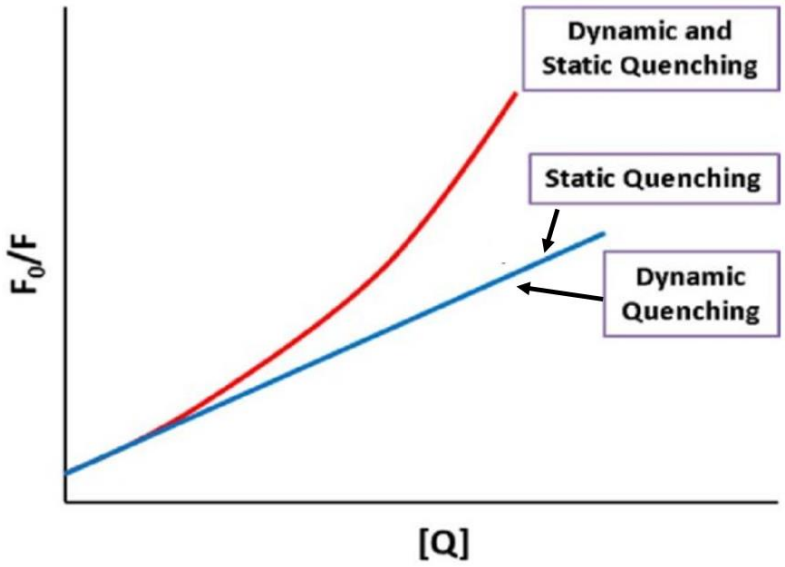


Figure 8 Stern-Volmer Plot showing the different forms of fluorescence quenching by a quencher, Q, static, dynamic and case when both types of quenching occurs

However, since the lifetime is unaffected by the presence of quencher in cases of pure static or pure dynamic quenching, a plot of $\tau_o/\tau$ versus [Q] would give a straight line. When the Stern-Volmer plot is linear, only one type of quenching occurs (Figure 8).

Fluorescence quenching has been widely studied both as a fundamental phenomenon, and as a source of information about biochemical systems. Due to the molecular interactions that results in quenching, biochemical applications of quenching is important. For either static or dynamic quenching to occur the fluorophore and quencher must be in contact. The requirement of molecular contact for quenching results in the numerous applications of quenching. For example, quenching measurements can reveal the accessibility of fluorophores to quenchers. Consider a fluorophore bound either to a protein or a membrane. If the protein or membrane is impermeable to the quencher, and the fluorophore is located in the interior of the macromolecule, then neither collisional nor static quenching can occur. For this reason quenching studies can be used to reveal the

localization of fluorophores in proteins and membranes, and their permeability to quenchers [101].

### 2.4.3 Synthesis of QDs

Bawendi and his coowokers suggested the first synthesis protocol of luminescent quantum dots in 1993 [103]. CdSe is commonly used because the synthesis is well-developed [104] and it covers the visible range which matches the detection range of most fluorescence detectors and imaging devices including CCD cameras, photomultiplier tubes (PMT), among others [3].

Methods for preparation of quantum dots can be conditionally divided into physical (no chemical transformation of matter occurs) and chemical ones (chemical reaction of formation of a substance as necessary step) [105]. Physical methods usually involve nucleation and growth of particles from the vapor phase. The one and only practically valuable, pure physical method for preparation of semiconductor quantum dots is molecular beam epitaxy [106] .The approach involves deposition from atomic or molecular beams produced by sublimation from some solid sources on crystalline substrates with atomically smooth surface in ultrahigh vacuum.

The synthesis of the most frequently used semiconducting colloidal QDs, consisted of metal chalcogenides (sulphides, selenides and tellurides), is based either on usage of organometallic precursors (e.g. dimethylcadmium [107], diethylzinc [108]), metallic oxide (e.g. CdO [109]) or metallic salts of inorganic and organic acids (e.g. stearate [110, 111], acetate [112, 113], nitrate [114]) which are chemical methods of synthesis. The sources of chalcogenide anion are usually pure halogen elements (e.g. S, Se, Te). Whatever precursor is used, the resulted QDs are hydrophobic, but their quantum yields (QY) are higher (in the range of 20–60 %) compared to QDs prepared by aqueous synthesis route (below 30 %).

However, the trend is to avoid the usage of organometallic precursors, because they are less environmentally benign compared to other ones, which are more preferable [115].

The second and more utilized way is the aqueous synthesis producing directly water soluble QDs with excellent biological compatibility and stability (usually more than two months). Compared with organic phase synthesis, QDs synthesized in aqueous way exhibit good reproducibility, low toxicity, and are less expensive. Basically, the fabrication process of water-soluble QDs takes place in reflux condenser.

This synthesis route usually consists in reaction of heavy metal (Zn, Cd, …) precursor with halogen precursors. Ordinary used precursors of heavy metals easily dissolving in water are acetates, nitrates or chlorides. The halogen precursors can be either commercial solid powders (e.g. $Na_2TeO_3$ in the case of CdTe QDs) or freshly prepared before using in reaction procedure, e.g. $H_2Te$ (preparation by adding sulphuric acid dropwise to the aluminium

telluride ($Al_2Te_3$) [116]) or NaHTe (forming by reaction of sodium borohydride ($NaBH_4$) with Te powder [117, 118]) in the case of CdTe QDs. However, NaHTe and $H_2Te$ are unstable compounds under ambient conditions; therefore the synthesis of CdTe QDs generally has to be performed in inert reaction systems. Since $Na_2TeO_3$ is air-stable, all of operations can performed in air, avoiding the need for an inert atmosphere. The synthetic pathway is thus free of complicated vacuum manipulations and environmentally friendly.

Nevertheless the procedure in water phase needs very long reaction time ranging from several hours to several days. Recently, new strategies employing microwave-assisted (MW) synthesis, which seems to be faster compared to the reflux one.

The other disadvantages of QDs synthesized through aqueous route are the wider FWHM (the full width at half maximum) and lower QY which can be attributed to defects and traps on the surface of nanocrystals [119]. These defects can be eliminated by the selection of capping agents. The process of functionalization involves ligand exchange with thioalkyl acids such as thioglycolic acid (TGA) [120], mercaptoacetic acid (MAA) [121], mercaptopropionic acid (MPA) [122, 123], mercaptoundecanoic acid (MUA) [124], mercaptosuccinic acid (MSA) [125] or reduced GSH [126, 127].

## 2.5 Bioconjugated Quantum Dots

One of the most important characteristic of QDs that has been researched is their bioconjugation with different biological molecules such as protein, peptides and nucleic acid [7]. By providing unique optical and magnetical properties QDs can facilitate detection and identification of biomolecules [128]. Shema of bioconjugation techniques are shown in Figure 9.

Bruchez [129] and Chan [94] were first to conjugate QDs to biomolecules in 1998 and since then this techniques has been greatly exploited in a variety of imaging, immunoassays and DNA sequencing technique.

There are two main approaches to immobilize biomolecule on a QDs surface: covalent linking and non-covalent binding, including coupling directly to the QD surface or surface ligand coating the QD [9]. Non-covalent attachment of biomolecules to the QD surface is mainly based on two types of QD surface-biomolecule interaction: electrostatic interaction (e.g. biotin/(strept)avidin). Simple non-covalent adsorption of the adsorption to the QD surface is the least demanding approach but the activity of the biomolecules can be compromised and there is no control over the orientation and valency of biomolecules. In most cases, noncovalent attachment arises by comparatively weak coordination binding, and consequently the stability is quite sensitive to the QD and biomolecule concentrations during preparation and in their application.

Covalent conjugation between QDs and molecules involves the reaction of the functional group with another, resulting in formation of a covalent bond. For QDs, the used

hydrophilization strategy determines which functional groups are present on the QD surface and this, subsequently, determines the covalent binding strategy. Covalent binding can be realized by use of functional crosslinkers. There molecules meant to join two (or more) molecule entities together: but they can also serve to introduce a new functional group, for example converting a QD-$NH_2$ to also display free thiols. Crosslinkers can differ in the amount of additional atoms (linker length) they add after bioconjugation and the nature of their functional groups. The smallest available crosslinkers for bioconjugation are so-called-zero-length crosslinkers (e.g. EDC and N, N'- Dicyclohexyl carbodiimide (DCC)).

The most well-studied and easy-to-perform method for attaching biomolecules to QDs makes use of the zero-length crosslinker carbodiimide such as EDC [130, 131] . Bioconjugation happens by direct formation of the amide bond between terminal carboxyls in the QDs and amines on the biomolecule (e.g. proteins), although the reverse configuration may work equally in some cases [132]. In general, EDC is cheap, easily obtained, and there are many protocols readily available for reference. However, single use of EDC often leads to a low yield because the reactive intermediate *o-acrylisoure*a tends to rapidly hydrolyze in aqueous solutions [133]. Therefore, in practice, EDC is often used in combination with water-insoluble NHS or water-soluble sulfo-NHS to form a stable active intermediate by converting it in an ester, increase solubility and increase the yield of conjugation [134, 135].

In general, the use of (strept)avidin binding to the biotin in molecule, 1-ethyl-3-(3-dimethylaminopyrol) carbodimiide hydrochloride (EDC) condensation as well as thiol-to-maleimide coupling strategies are more common due to the fact that these protocols have been well established in biology [136].

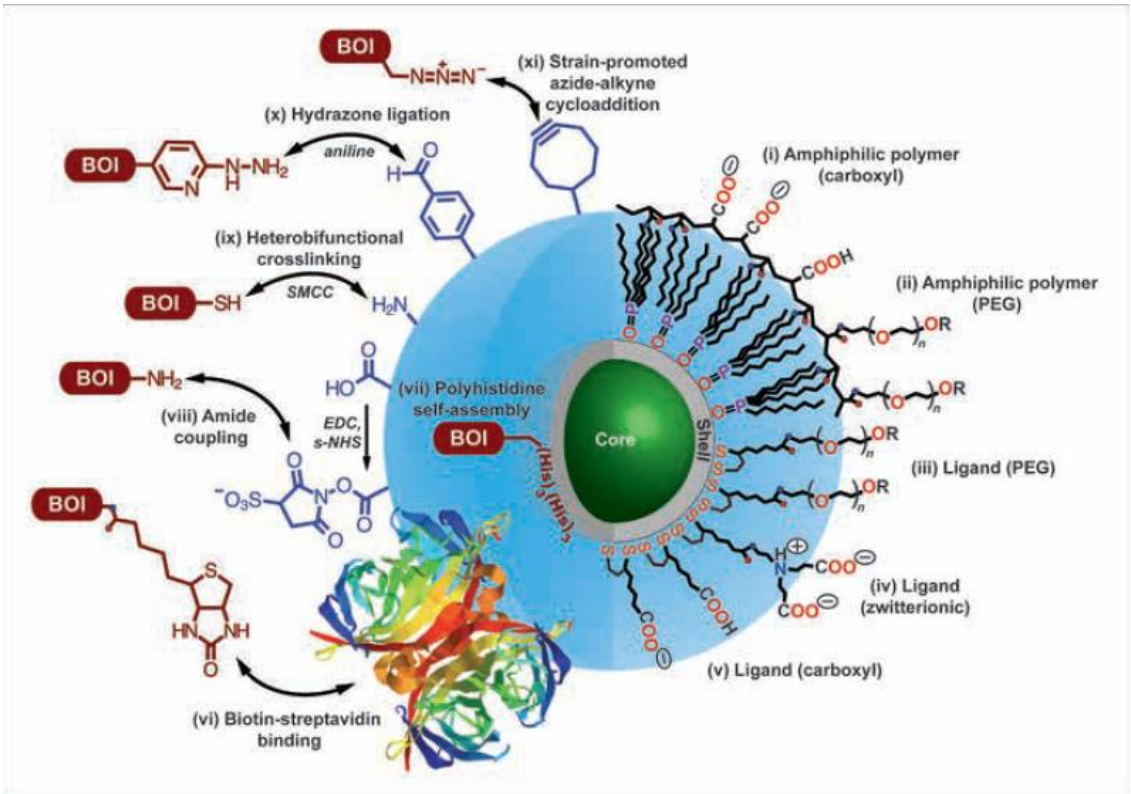


Figure 9 Illustrative overview of the chemistry of core-shell QDs. Coatings for aqueous solubility are as follows: (i) amphiphilic polymer coating with carboxyl(ate) groups; (ii) amphiphilic polymer coating with PEG oligomers; (iii) dithiol ligand with a distal PEG oligomer; (iv) dithiol ligand with a distal zwitterionic functionality; and (v) dithiol ligand with a distal carboxyl(ate) group. Common R groups include carboxyl, amine, and methoxy, although many others can be introduced (e.g., see vi, x, xi). Methods for conjugating biomolecules of interest (BOI) are as follows: (vi) bioti-streptavidin binding; (vii) polyhistidine self-assembly to the inorganic shell of the QD; (viii) amide coupling using EDC/s-NHS activation; (ix) heterobifunctional crosslinking using succinimidyl-4-(N-maleimidomethyl)cyclohexane-1-carboxylate (SMCC; structure not shown); (x) aniline-catalyzed hydrazone ligation; and (xi) strain-promoted azide–alkyne cycloaddition. The double arrows are intended to represent conjugation between the functional groups and, in principle, their interchangeability (not reaction mechanisms or reversibility). Not drawn to scale.

The following two proteins were selected for this study: bovine serum albumin (BSA) and mouse immunoglobulin G (mIgG). These model proteins were chosen with respect to the reliable, specific and selective immunoreactivity with appropriate antibodies exhibiting low cross-reactivity. Moreover, significantly different properties (molecular mass and pI) ensure optimal electrophoretic behavior for development and optimization of the method.

### 2.5.1 Bovine serum albumin

Bovine serum albumin (BSA) is a serum albumin protein derived from cows. It is often used as a protein concentration standard in lab experiments. Number of amino acid residues on BSA is 583, molecular weight 66,463 Da and isoelectric point in water at $25^0$C is 4.7. BSA has a similar composition of human serum and due its properties that is small, stable and moderately non-reactive protein, it has a number of application in immunology, biochemistry and biotechnology.

BSA immunoassay applications include ELISA (Enzyme-Linked Immunosorbent Assay)[137], immunoblots [138] and immunocytochemistry [139]. BSA is also used as a nutrient in cell and microbial culture. In molecular biology BSA is used to stabilize some restriction enzymes during digestion of DNA and to prevent adhesion of the enzyme to reaction tubes, pipet tips, and other vessels. BSA is considered to be a universal blocking reagent in many applications [140]. This is because BSA does not affect the functions of other proteins (enzymes) that do not need it for stabilization. BSA is also commonly used to determine the quantity of other proteins, by comparing an unknown quantity of protein to known amounts of BSA. BSA is used because of its stability to increase signal in assays, its lack of effect in many biochemical reactions, and its low cost, since large quantities of it can be readily purified from bovine blood, a byproduct of the cattle industry.

### 2.5.2 Immunoglobulin G

Immunoglobulin G (IgG) is the simplest, most abundant antibody class in vertebrates constituting some 75% of total immunoglobulin in humans. These molecules are glycoproteins formed of four polypeptide chains, consisting of two identical copies of each of two kinds of polypeptide chain: light (L) (which may be of either the κ or λ class), and heavy, gamma (γ) (which may be of one of four subclasses), linked together by disulfide bonds and noncovalent forces in the form L–H–H–L [141]. The resulting tetramer has two identical halves, which together form the Y-like shape (Figure 10). Individual immunoglobulin G molecules will differ in their amino acid sequence but within an IgG molecule the two L chains are identical and the two H chains are identical to each other, a consequence of the fact that only one L chain gene and one H chain gene is expressed in any antibody-producing cell [141].

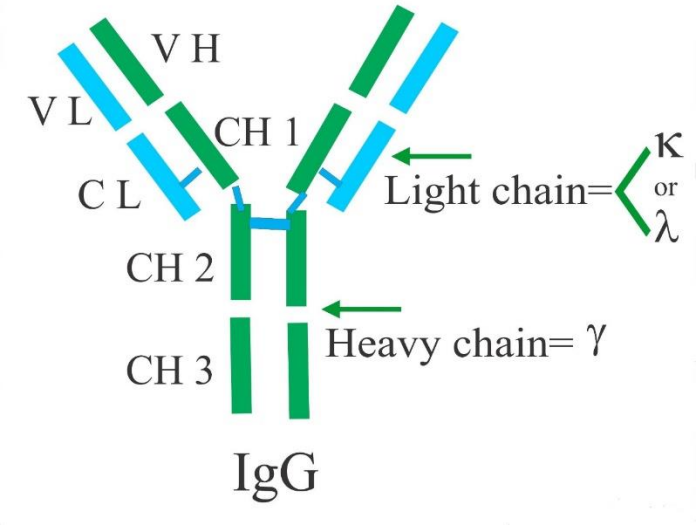


Figure 10 The various regions and domains of a typical IgG

IgG antibodies are large globular proteins with a molecular weight of about 150 kDa. The function of the molecule is to effect a liaison between antigen and the effector systems of the body. It is a multifunctional molecule, bivalent with respect to antigen, structurally differentiated with the antigen-binding sites at one end, one in each Fab, and a variety of sites for engaging nonspecific effector functions in the Fc region of the molecule [142].

### 2.5.3 Confirming bioconjugation

The confirmation of bioconjugated QDs is a very important stage in the proposed study. It must follow any newly started conjugation procedure, in order to be sure we actually have a quality conjugate. Due to attached biomolecules, bioconjugated quantum dots are characterized with increased size/volume/weight, which makes it possible to employ different separation technique for bioconjugation verification.

In our literature research, we find several bioconjugation verification methods/procedures that are currently available. The most popular one are different variations of gel electrophoresis [143-146]. The other two most widely used one are variations of capillary electrophoresis [7, 147, 148]and protein microarrays [149].

Gel electrophoresis is a simple method to separate the substances by size and charge in the electric field. Separation is in this case done in gel media. So *at el*, used this method to successfully confirm bioconjugation of CdSe/ZnS QDs to Luc-8 antibodies [143].

Protein microarrays are mostly used to employ bioconjugates for the antigen detection [150], but results have been reported that this method is successfully used to confirm bioconjugation as well.

Capillary electrophoresis as a mentioned in chapters above is a technique which can be used to separate ionic species by their charge and size. The separation takes place interior

of a small capillary filled with an electrolyte, and the detection in based on the photoluminescence of QDs. Capillary electrophoresis with laser-induced fluorescence detection (CE-LIF) has been used for characterization of the surface modifications of QDs and evolution of the particle charge [6, 46, 49]. Hung et al. demonstrated how simple optimization of pH of buffer can substantially improve the separation of CdTe QDs and their conjugates with an antibody [6].

In our work we used on a chip electrophoresis. This method is characterized with simplicity, small sample and reagent requirements, and high efficiency of separation.

### 2.5.4 Bioconjugated QDs applications

The development of high-sensitivity and high-specificity probes that lack the intrinsic limitations of organic dyes and fluorescent proteins is of considerable interest in many areas of research, from molecular and cellular biology to molecular imaging and medical diagnostics. QDs are believed to overcome these limitations That is the reason why, among the most successful applications in the implementation of quantum dots (QDs), is as highly fluorescent probes in molecular diagnostic [151].

QDs, in particular, have emerged as one of the most promising labels for immunoassay detection because if their photostability and size tunable photoluminescence. Application of QDs as fluorescence label in immunoassay was reported by Feng et al, QDs were first conjugate with antibody then separated by CE form free antibody and antibody-antigen complex [46]. They can be used to develop enzyme linked-immunosorbent assays (ELISAs) [152], lateral flow immunoassays (LFIAs) [153], Western blots [154] or in FRET studies [155, 156], to name but a few. For biosensing, the greatest potential of QD-conjugates lies in multiplexing [153, 157]. QDs play also an important role in in-vitro and in-vivo cell imaging [158], in-vivo drug delivery, are often used for cellular labeling (cell surface markers and intracellular markers) and have also made a lot of progress and attracted great interest in this area [159]. These applications are all possible because of the QDs versatile surface chemistry and bioconjugation. The type of bioconjugation should be selected carefully depending on the goals and application.

Although the case for using QD-based fluorescent labels is compelling, it should be noted that QDs are not likely to replace organic dyes in all biological applications. Some of the challenges that have yet to be overcome include economic factors: QDs are expensive in comparison to organic dyes, and there is an initial investment required for researchers and instrument suppliers to produce systems optimized for use with QDs. Also, probe size and steric hindrance must be examined when assessing the suitability of a QD based approach to fluorescent labeling of molecules. Since QDs are an order of magnitude larger than organic dyes, the extent to which their presence perturbs the biological process being observed must be determined. This is particularly important when multicolor experiments are desired, since labeling several biomolecules with QDs of different sizes could result in varying degrees of perturbation due to the large differences in the QD sizes. In contrast,

most organic dyes are of similar size in spite of their large differences in absorption/ emission characteristics [160].

QDs were considered to be safe for living organisms, still the question about QD's toxicity has been rising by many groups. QDs have been found to cause vascular thrombosis in the pulmonary circulation [87], could induce apoptosis and cell death [88], and may accumulate in the lungs, spleen, liver and kidneys [89]. Therefore, QDs may not be as safe for humans, as previously reported. This factor is especially important for the in vivo QD applications (bioimaging, drug delivery), as in this case, QDs are injected into humans directly. In-vitro applications of QDs could also be affected, but at least these issues may be solved with the proper precautions measures (wearing protective equipment, washing hands etc).

To summarize, although QDs may look very promising as novel fluorescent biomarkers, there are still many issues to be overcame for them to be widely used in clinics.

# 3. AIMS OF THE THESIS

Taking in consideration scientific importance for solving problems in bioconjugation of QDs and their separation and detection with on a chip platforms, aim of this thesis is to seek for best bonding technique between QDs and biomolecules and to detect multiple biomolecules using CE immunoassay. This aim can be divided into few objectives to be solved:

1. Choosing and testing suitable procedure for synthesis of QDs
2. Propose the appropriate strategy for conjugation of QDs with biological molecule
3. Evaluate performance of the proposed conjugation techniques
4. Developing in our laboratory electro-optical system for the separation and fluorescence detection of bioconjugated QDs
5. Studying of QDs luminescence quenching effect caused by covalent conjugation with protein using on a chip CE
6. Evaluate performance of electro-optical system on a chip using a multi-analyte immunoassay based on quantum dots (QDs) fluorescence

# 4. EXPERIMENTAL METHODS

## 4.1 Synthesis of CdTe QDs capped with MPA

The procedure for synthesis of MPA-capped CdTe QDs was adapted from the work of Long *et al.* [161]. $CdCl_2$ (183 mg) and 400 mg trisodium citrate were dissolved in 90 $cm^3$ of water, followed by the addition of 104 $mm^3$ of MPA. The pH of the solution was adjusted to 10 using 1 mol $dm^{-3}$ NaOH. 44 mg of $Na_2TeO_3$ and 100 mg of $NaBH_4$ were added to the solution under vigorous stirring. The mixture was kept at 95 °C under the reflux cooling (Figure 11) a specific time (depending on the size of QD that we expected to achieve) for 1 and 2 hours for green and orange respectively.

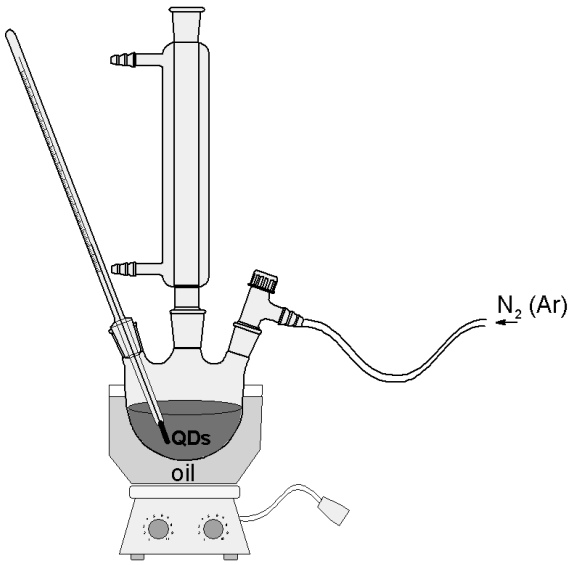


Figure 11 Schema of apparatus for QDs preparation in reflux condenser

## 4.2 Preparation of QDs conjugates via CDI, EDC, EDC/NHS

In this work, we used so called zero-length-cross-linking agents: CDI, EDC and EDC with addition of NHS, as coupling agents.

In order to produce BSA QDs conjugates, in first experiment we used CDI (10 $mm^3$, 10 mmol $dm^{-3}$) containing PBS buffer (100 mmol $dm^{-3}$, pH 7.4) and added to the solution of orange CdTe QDs (1000 $mm^3$, 1 mg $dm^{-3}$). The solution was incubated at room temperature for 30 min to activate carboxyl groups. Then, different concentration BSA (200 $mm^3$; 7.52 ×

$10^{-8}$, $1.50 \times 10^{-7}$, $3.00 \times 10^{-7}$, $4.51 \times 10^{-7}$, $6.00 \times 10^{-7}$, $7.52 \times 10^{-7}$, $1.31 \times 10^{-6}$, and $1.50 \times 10^{-6}$ mol $dm^{-3}$) was added to the solution and incubated at room temperature for 2 h [162]. During the reaction of carboxyl groups on the surface of QDs with CDI, a reactive intermediate, N-acylimidazole, is formed with liberation of carbon dioxide and imidazole as innocuous side products. The N-acylimidazole can then react with amines form stable covalent amide or ester linkages, respectively (Figure 12) [33].

For producing BSA QDs conjugates in second experiment we used BSA (250 $mm^3$; $7.52 \times 10^{-8}$, $1.50 \times 10^{-7}$, $3.00 \times 10^{-7}$, $4.51 \times 10^{-7}$, $6.00 \times 10^{-7}$, $7.52 \times 10^{-7}$, $1.31 \times 10^{-6}$, and $1.50 \times 10^{-6}$ mol $dm^{-3}$) and EDC (57 $mm^3$, 10 mg $cm^{-3}$) and added to the solution of orange CdTe QDs (250 $mm^3$, 0.1 mg $cm^{-3}$). The solution was then incubated at room temperature for 2 h [163]. 1-Ethyl-3-(3-dimethylaminopropyl)carbodiimide(EDC) reacts with a carboxyl group of QDs to form an amine-reactive O-acylisourea intermediate, which is highly unstable and short-lived in aqueous solution (Figure 12). Thus, hydrolysis is a major competing reaction [34].

It was found that the addition of sulfo-NHS stabilizes the amine-reactive intermediate by converting it to a semi-stable amine-reactive sulfo-NHS ester, thereby increasing the efficiency of EDC mediated coupling reactions (Figure 12) [15].

For producing another type of BSA QDs conjugates we added EDC (200 $mm^3$, 50 mmol $dm^{-3}$) and sulfo-NHS (200 $mm^3$, 5 mmol $dm^{-3}$) to the solution of orange CdTe QDs (200 $mm^3$, 0.1 mg $cm^{-3}$). The solution was incubated at 32 °C for 30 min. Then, BSA (200 $mm^3$; $7.52 \times 10^{-8}$, $1.50 \times 10^{-7}$, $3.00 \times 10^{-7}$, $4.51 \times 10^{-7}$, $6.00 \times 10^{-7}$, $7.52 \times 10^{-7}$, $1.31 \times 10^{-6}$, and $1.50 \times 10^{-6}$ mol $dm^{-3}$) was added to the solution and incubated at 32 °C for 2 h while shaking [164].

For synthesis of QDs conjugated to antibody and antigen, method described in further text was used.

Mixture of EDC (200 µL, 50 mM) and sulfo-NHS (200 µL, 5 mM) were added to the solution of both orange and green CdTe QDs (200 µL, 0.1 mg $mL^{-1}$). The solution was incubated at 32 °C for 30 min. Then, different concentration of 200 µL anti-BSA, was added to the solution of green QDs and 200 µL with different concentration anti-IgG was added to orange QDs and incubated at 32 °C for 2 h while shaking. This conjugation procedure is simple, fast and selective to carboxyl groups on the QD surface and primary amino groups of a protein. After formation of QDs-antiBSA and QDs-antiIgG, BSA and mouse IgG were added while shaking at the room temperature. The resulting solution contained stable QDs-immunocomplex without obvious aggregates and was ready for assay.

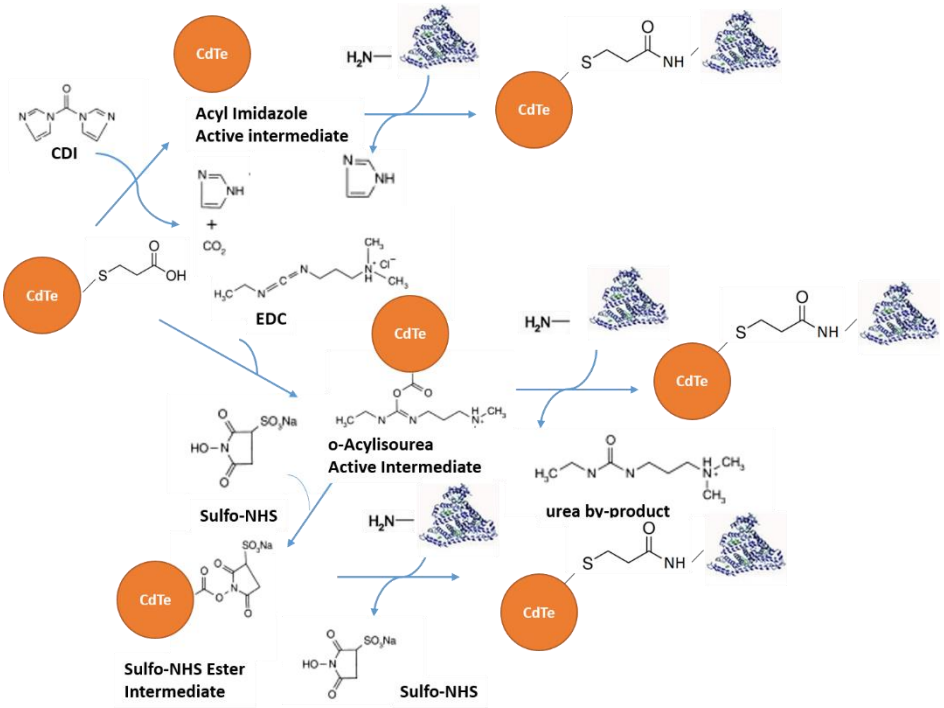


Figure 12 Bioconjugation reaction scheme of CdTe–MPA QDs to BSA

## 4.3 Equipment used for characterization of pure QDs and their conjugates

### 4.3.1 Measure of Fluorescence

Fluorimetric analysis was performed using multifunctional microplate reader Tecan Infinite 200 PRO (TECAN, Switzerland). 380 nm was used as an excitation wavelength and FL scan within the range from 420 to 800 nm was measured with 2 nm steps. Each intensity value is an average of five measurements. The detector gain was set to 60. 200 $mm^3$ of the sample (QD–BSA conjugates coupled via CDI, EDC or EDC/sulfo-NHS, CdTe–MPA QDs) was placed in transparent 96 well microplate with flat bottom by Nunc (Thermo Scientific, USA).

### 4.3.2 Dynamic light-scattering measurements

Dynamic light-scattering measurements were recorded on the DynaProNanoStar (WYATT Technology, USA). The measurements were performed at constant temperature (25 °C) in disposable plastic cuvette. Samples were filtered through a 0.22 mm membrane filter prior to measurements. The light source was an argon-ion laser (DynaPro NanoStar, Wyatt Instrument Technology, λ = 658 nm) and photons scattered by the sample were collected at angle 90°, multi-tau correlator was used for analysis of diffusion coefficients resulting in micelle size, and dynamics software was employed to results evaluation. $d_{hydr}$ was calculated from the translational diffusion coefficient using Stokes–Einstein equation.

## 4.4 CE chip fabrication

To decrease the analysis cost as well as carryover effect, a single-use polymeric microfluidic chips were used in this study.

The easy and reliable production suitable for large-quantity preparation increased the reproducibility of the analyses due to the minimization of errors caused by lithographic procedure.

Rapid prototyping of a chip starts with creating design for a device in a computer/aided design software. A high-resolution printing is used to print design on a chrome transparency mask. This transparency serves as a photomask in photolithography to produce a positive relief of photoresist on silica wafer. Silica mold with channels of 50 µm width was made and used for rapid molding of PDMS.

### 4.4.1 Lithography

Photolithography was used to fabricate mold with microchannels. Next steps were performed to fabricate mold with channels (Figure 13) :

1. A blank 100 mm diameter Silicon wafer (Si (100) wafer, n-type, 500nm of $SiO_2$ layer) was rinsed with isopropyl alcohol, deionized water, and dried with $N_2$ gun. To increase adhesion of photoresist on the silicon wafer, surface was treated with Hexamethlyldisilazane (HDMS) for 5min.
2. AZ 1518 positive photoresist was spinned (2-step spinning parameters : step one- 500 rpm, 5sec; step two- 4000 rpm, 45sec) to create uniform film ~ 2µm thick. Wafer was pre-bake on a hot plate (100$^{O}$C for 2 min).
3. Wafer was exposed with 2500 mJ/cm$^2$ at 405 nm through a photomask. Post/bake was done at 200$^{O}$C for 1 min. Wafer was developed in AZ 327 for 40 sec, rinsed in isopropanol and dried with $N_2$ gun.
4. Etching of silicon dioxide, to remove areas of silicon dioxide unprotected by photoresist,

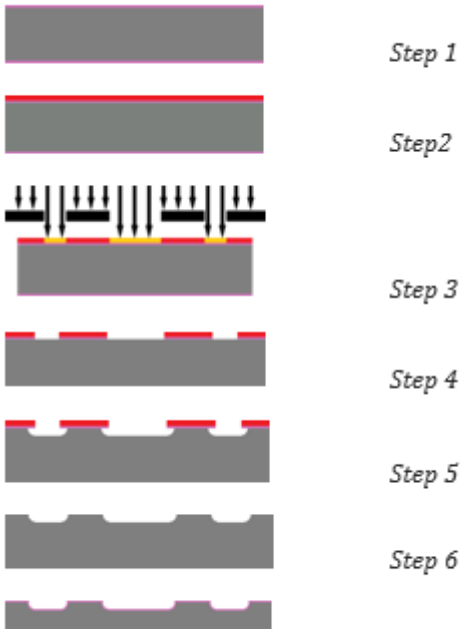


Figure 13 Lithography steps for fabrication of silica mold

was done using buffered oxide etch (BOE) solution (6 parts of 40% $NH_4F$ and 1 part of 49% HF) for 20 sec.

5. $XeF_2$ was used for dry isotropic etching of silicon.

6. Rinsing with isopropyl alcohol was done to remove photoresist. Polishing of surface of wafer with microchannel was done using mixture of $HNO_3$ and BOE (buffered oxide etch) (100:1).

7. Wafer mold was cleaned using piranha solution(mixture of sulfuric acid ($H_2SO_4$ and hydrogen peroxide $H_2O_2$) for few seconds.

### 4.4.2 PDMS molding

A mixture of the PDMS prepolymer and curing agent at a ratio of 10:1 (w/w) was completely degassed and poured onto the silica mold, which was cured for 2 h at 65 °C, and peel off. After air drying of channels, PDMS is punched to make holes (2 mm) as fluid reservoirs. The patterned side of the PDMS was treated with oxygen plasma (200 W, 15 min) and bonded permanently with a plasma-treated glass substrate to form a closed fluidic system (Figure 14). The microfluidic chip contained fabricated channels ≈50 µm width and ≈5 µm depth. The chip design is shown in Figure 15.

./ 9999

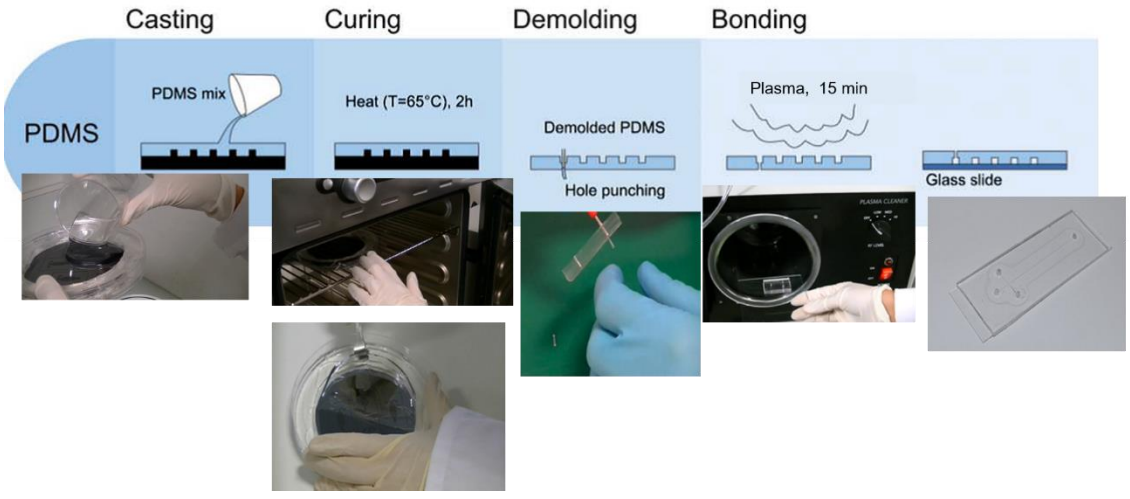


Figure 14 Creating of PDMS-glass microfluidic chip

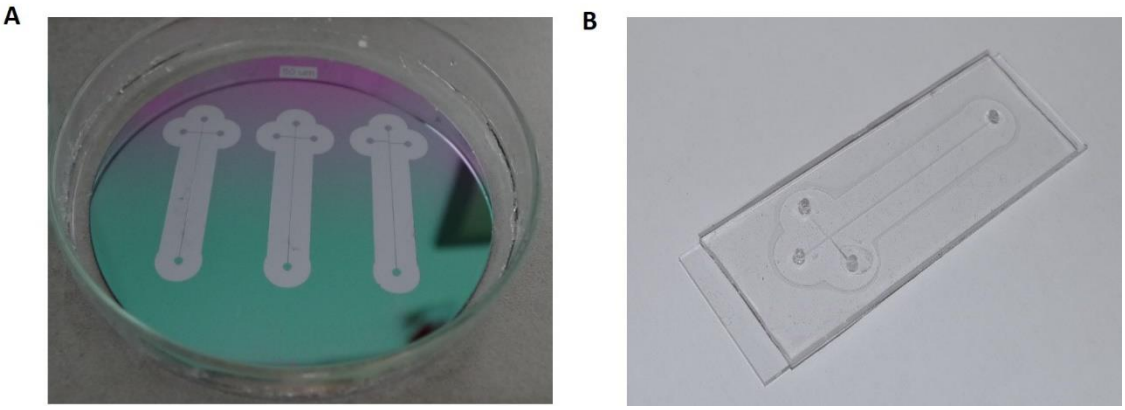


Figure 15 A) Fabricated mold with microchannel B) final look of fabricated chip

## 4.5 PDMS surface treatment

When using polymer care must be taken in control of surface chemistry. One of the main disadvantages of using PDMS channel, is that walls are not natively charged, and those cannot produce strong EOF, which is necessary to move analytes toward detector as well as to electro-kinetically manipulate fluid flow [165]. Low thermal conductivity of PDMS can lead to rise in temperature due to resistive heating in electrophoresis. This rise in temperature causes broadening of peaks and lowers the resolution of system. Also adsorption of hydrophobic analytes into native PDMS, has been reported [166]. To overcome this problem modification of PDMS is necessary. Surface of PMDS can be either dynamically or permanently modified. Dynamic coatings such as SDS, or TTAB [167], oxidation with plasma[168] and covalent modification [169].

In our work the patterned PDMS side was exposed to oxygen plasma for 15 minutes and surfactant Tween 20 was added to a running buffer.

Results of separation of CdTe QDs conjugated with BSA, using on a chip CE, before and after PDMS surface treatment was shown in Figure 16. Clearly it can be noticed that no surface treatment results in broad peak and poor separation resolution.

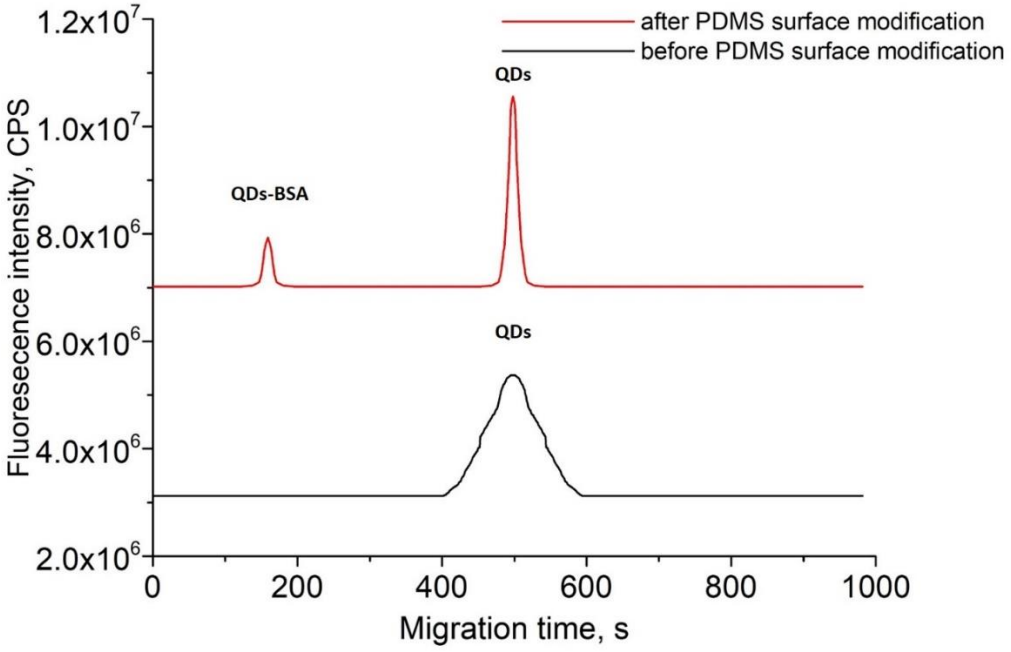


Figure 16 Electropherograms of separation of the QDs and bioconjugated QDs with BSA, before and after surface plasma modification of PDMS chip

Exposing PDMS replica to plasma introduces polar groups on the surface. Plasma introduce silanol groups (Si-OH) at the expense of methyl groups (Si-$CH_3$) [170]. This silanol groups condense with appropriate groups (OH, COOH, ketone…) on another surface, when they are brought together. In PDMS-glass contact these are SiO-Si bonds. These covalent bonds make tight, irreversible seal. As already mentioned PDMS has hydrophobic surface. This surface is hard to wet with other aqueous solutions, and making adsorption of other hydrophobic species as well as nucleate bubbles. Exposure to plasma makes surface more hydrophilic due to presence of silanol groups. Due to this aqueous solution can easily wet surface of channel, this also makes on the walls of channel ioniziable groups ($SiOH \leftrightarrow SiO^- + H^+$). These groups will in contact of basic and neutral solutions support strong EOF toward cathode. Nevertheless, this negatively charged channels have great resistance to adsorption of hydrophobic and negatively charged analytes. When using this process care must be taken in choice of a gas, timing after plasma, and cleanliness.

When using PDMS chip for separation of bioconjugated QDs adsorption of biomolecule was observed which was resulting in broad peak and poor separation resolution. To overcome this problem in our work surfactant Tween 20 was used. Surfactant is added into the running buffer to achieve the hydrophilic PDMS surface. The hydrophobic tails of the amphiphilic surfactant molecules were adsorbed onto the PDMS surface while the hydrophilic heads stick out in the buffer, thereby changing the PDMS surface properties. In this way, surface modification can be accomplished faster, cheaper and simpler [171] .

## 4.6 Instrumental set up and data acquisition

On a chip electrophoresis were carried out using a developed electro-optical system. The system consists of the five parts: light source, sample holder, light detector, control electronics and high voltage generator. Excitation light is generated by ultraviolet light-emitting diode (UV LEDs Roithner Laser Technik GmbH, λmax = 375 nm, output power 5.5 mW) and filtered by optical 380 nm low-pass filter (BAADER U-Filter No.: 2458292). This light excites FL of the sample and emitted light is selected by 420–680 nm high-pass optical filter (BAADER UV/IR-Cut/L filter No.: 2459207A) and https://www.edmundoptics.com/p/520nm-cwl-10nm-fwhm-125mm-mounted-diameter/20157/. This emitted light is detected by photodetector including photomultiplier (Perkin Elmer, MP 963, spectral response 185–850 nm).The system is powered from low voltage source Agilent and sample flow control is provided by linear syringe pump. The applied voltage for the electrophoretic separation was ≈3 kV. This high voltage was generated from 5V voltage source.

The prepared microfluidic chips were connected to the small laboratory-made electrophoretic system employing light emitting diode as a miniaturized, low-energy consuming and low-cost excitation source. The system was equipped with a special optical filter holder enabling simple filter replacement and miniaturized photomultiplier tube for signal detection. Optical part with chip were placed into black box to avoid room light interference and insensitivity to temperature changes. The photograph of the instrumental set up as well as the scheme of connection of all necessary components are shown in Figure 17.

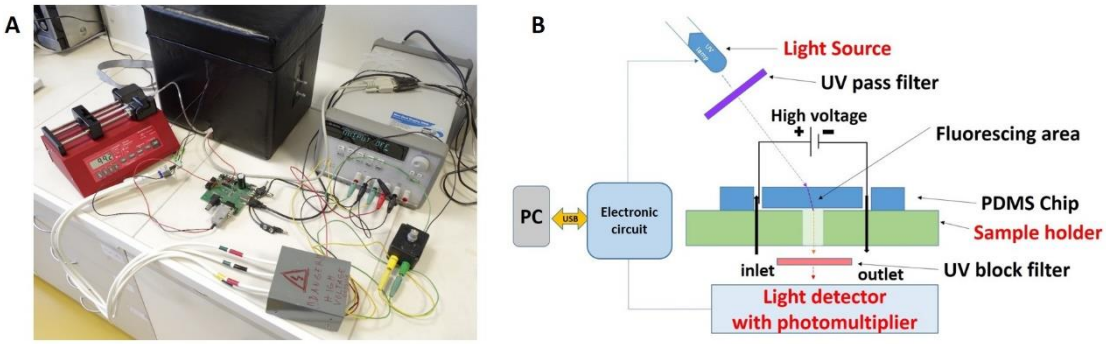


Figure 17 A) Photograph of the experimental setup, syringe pump, and power supply. B) Scheme of the electro-optical system

### 4.6.1 CE procedure

The fabricated chip is placed on the sample holder (Figure 18) and microchannels are first filled with buffer. 100 µL of sample, prepared as mentioned above, was loaded in inlet reservoir. After filing the sample reservoir, platinum electrodes are placed in each fluid reservoir and contacted to power supplies. CE separation was accomplished with an effective length of ≈8 cm between inlet and detector (total chip length ≈10 cm). Initially a new chip was flushed with 0.1 mL NaOH (10 min), water (10 min), and running buffer (10 min). 10 mL Borate buffered saline buffer (BBS, pH ≈9.14) was used as a BGE. The mobility of the EOF, which transported analytes from the injection reservoir to the detector at the negative voltage, was determined using coumarin as a neutral marker. All solutions were filtrated through a 0.45 µm membrane filter before use. The read out from electronics was sent to laptop, and application enabling to save data in excel file was used.

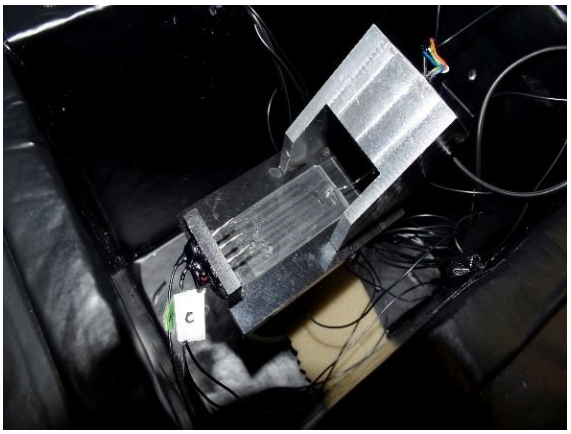

Figure 18 The prepared microfluidic chips connected to the laboratory-made electrophoretic system

## 4.7 Characterization of QDs and their conjugates

### 4.7.1 MPA coated QDs characterization

Water-soluble CdTe QDs were synthesized and stabilized with 3-mercaptopropionic acid (MPA). QDs used in this study showed narrow and symmetrical emission spectrum excited at 380 nm on multimode microplate Tecan reader. It was found that FL intensity is increasing with increasing of reaction time and the red shift was observed. QDs exhibit a strong emission of red light with emission maximum at 600 and 76 nm of full-width at half-maximum (FWHM) after 4 h of reaction (Figure 19). The sample with reaction time of 4 h showed the highest FL and was chosen for further conjugation with protein. The absolute quantum yield of QDs was evaluated to be 16.5% by Quanta u quantum yield measurement system (FluoroLog, HORIBA Jobin–Yvon). The ‘‘blank experiments’’ using bioconjugation agents (CDI, EDC, and sulfo-NHS) and BSA were done to be sure that there is no contribution

of side products to luminescence of system (Figure 19).

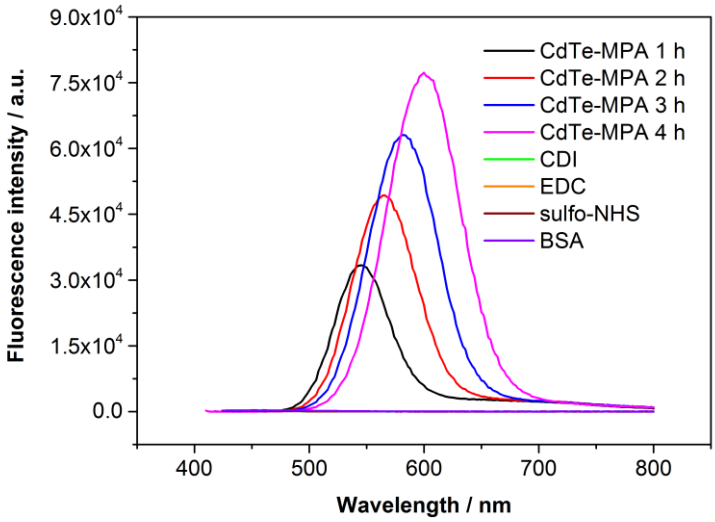


Figure 19 Emission spectra of MPA-capped CdTe QDs at different reaction times: 1, 2, 3, and 4 h; pure CDI, EDC, sulfo-NHS and BSA, and excitation wavelength at 380 nm

The crystal structure of CdTe QDs was examined with powder X-ray diffraction (XRD) on Empyrean X-ray diffractometer, PANalytical. The XRD pattern of CdTe QDs shows diffraction peaks at positions $2\Theta \approx 24^0$, $40^0$, and $46^0$ which are indexed corresponding to prominent orientation (111) and two other weak orientations (220) and (311), respectively (Figure 20). These confirm that synthesized CdTe is in cubic zinc blende structure and lattice is face-centered system. The intensity of XRD peak indicates that synthesized CdTe QDs are crystalline and broad diffraction peaks indicate very small-sized crystals [172].

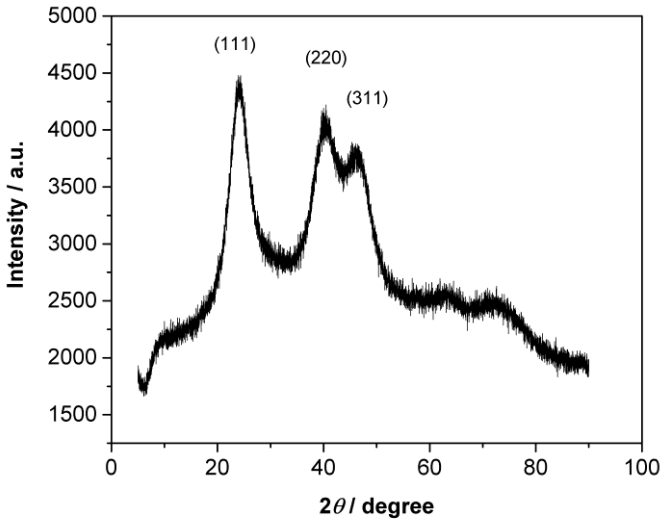


Figure 20 X-ray diffractogram of powder pattern of MPA-capped CdTe QDs

Dynamic light-scattering (DLS) measurements were performed to determine the hydrodynamic radius of QDs before and after conjugation with protein. The hydrodynamic diameter ($d_{hydr}$) of CdTe–MPA QDs was found to be (2.8 ± 0.5) nm and represents mean value ± standard deviation and three measurements. There is a significant increase in diameter size after conjugation. This confirms the successful conjugation of a protein on a surface of QDs. When using EDC/sulfo-NHS as a cross-linker and after BSA coating, dhydr was determined as (7.1 ± 0.1) nm (mean value ± standard deviation, 3 measurements) which perfectly correlates with the literature [28]. MPA- and protein-conjugated CdTe QDs are well dispersed in phosphate-buffered saline (PBS) buffer, and there were no agglomerates or formed clusters of several QDs. Table 2 summarizes the data from DLS measurements.

Table 2 Hydrodynamic diameters of CdTe–MPA QDs before and after bioconjugation with BSA using different cross-linkers, determined by DLS

| Type of cross-linker | $d_{hydr}$/nm (mean value ± standard deviation) | |
|---|---|---|
| | CdTe-MPA | CdTe-MPA-BSA |
| CDI | | 5.5 ±0.1 |
| EDC | 2.8 ± 0.5 | 5.8 ±0.1 |
| EDC/sulfo-NHS | | 7.1 ±0.1 |

### 4.7.2 Conjugated QDs characterization

In this work, so called zero-length-cross-linking agents were used as coupling agents. Two step procedure combining EDC with sulfo-NHS that conjugates carboxyl and amine groups to form stable covalent amide linkages was used.

The optical properties of QDs are strongly dependent on their size which can be easily controlled by the time of synthesis. Therefore, two types of CdTe QDs differing only in the size were conjugated with two different antibodies. The optical characteristics of the bioconjugated QDs are shown in Figure 21. Narrow and symmetrical emission spectra were observed when excited by 350 nm. It clearly follows from these results that the emission maximum of the anti-BSA-modified CdTe QDs is at 532 nm (green emission), while the emission maximum of the anti-IgG-modified CdTe QDs is at 610 nm (orange emission). The photograph of the solutions of bioconjugated QDs under UV light illumination is shown in the inset in Figure 21A

Bioconjugation reaction scheme of CdTe–MPA QDs to anti-BSA and anti-IgG via covalent coupling is shown in Figure 21C. First, CdTe–MPA QDs were prepared in aqueous solution phase. The thiol group of MPA is linked to the surface of CdTe QDs by thiol group-Cd coordination, and the functional carboxylic group is free, which can be easily coupled to biomolecules with amino groups, such as proteins, peptides, and amino acids. So-called zero-length-cross-linking agents and two-step procedure combining EDC with N-hydroxysulfosuccinimide (sulfo-NHS) was used as a coupling agent, that conjugate carboxyl groups and amines to form stable covalent amide linkages.

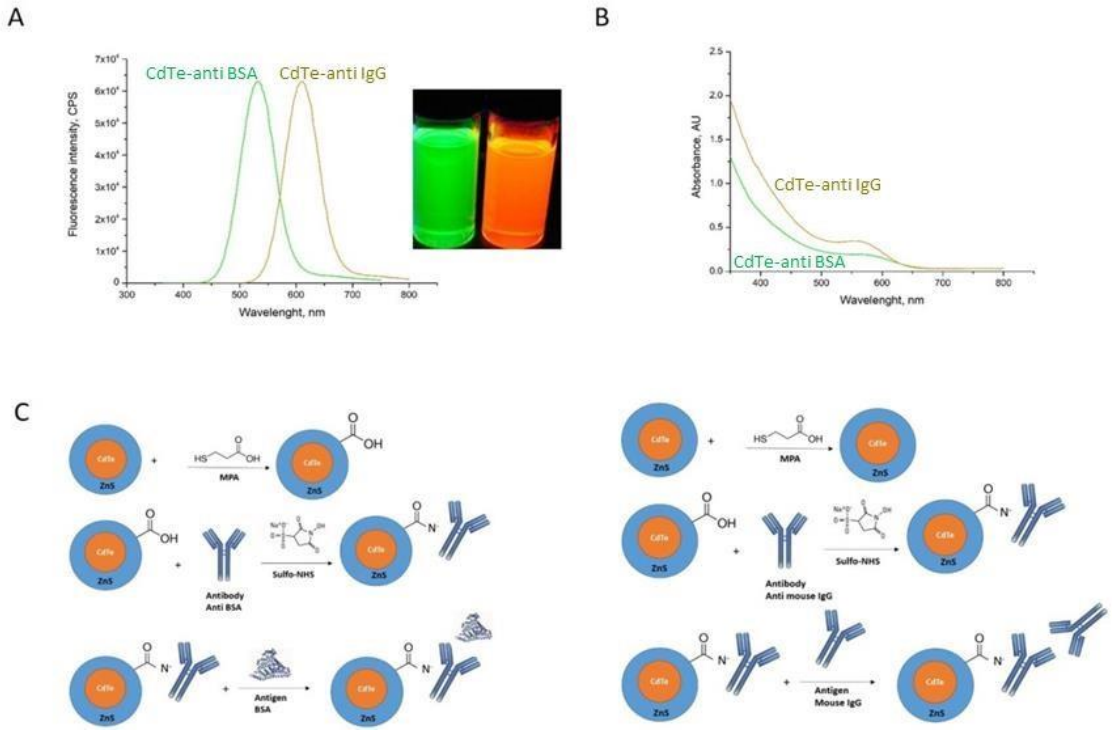


Figure 21 Characterization of quantum dots. A) emission spectra of bioconjugated QDs inset: photograph of QDs solution under UV light illumination, B) absorption spectra of bioconjugated QDs, C) Bioconjugation reaction scheme of CdTe–MPA QDs to anti-BSA (left) and anti-IgG (right)

### 4.7.3 Determination of the charge density at the surface of QD

The surface charge density *r* of a spherical particle in electrolyte solution can be calculated using following formula introduced by Ohshima [173]:

$$\sigma = \frac{2\varepsilon_r\varepsilon_o\kappa kT}{e}\sinh\left(\frac{y}{2}\right)\left[1+\frac{1}{\kappa a}\left(\frac{2}{\cosh^2(y/4)}\right)+\frac{1}{(\kappa a)^2}\left(\frac{8\ln[\cosh(y/4)]}{\sinh^2(y/2)}\right)\right]^{\frac{1}{2}} \quad (9)$$

where $\varepsilon_r$ and $\varepsilon_o$ are the relative and vacuum dielectric constants respectively, *e* is the elementary electric charge, $\kappa$ is inverse Debye thickness, a is hydrodynamic radius, *k* is the Boltzmann constant, T is thermodynamic temperature and parameter y= e ζ/kT.

QDs emission maximum and their dimeter, pH and ionic strength of background electrolyte (BGE) that were used for CE, were also used for calculations of respective inverse Debye thickness $\kappa$ based on Voráčová et al. [174]. For a calculation of ζ-potential of

synthesized QDs, electrophoretic mobility was used, which was measured using neutral marker, as explained in experimental part. The surface charge of synthetized MPA-QDs according to (7) was calculated to be -0.0155 C $m^{-2}$.

# 5. STUDYING OF QUANTUM DOT LUMINESCENCE QUENCHING EFFECT CAUSED BY COVALENT CONJUGATION WITH PROTEIN

## 5.1 On-a-chip electrophoresis of bioconjugated QDs

Binding of QDs with biomolecules can be determined by measuring the changes in the electrophoretic mobility overtime of bioconjugated QDs by CE, since interaction with these molecules will result in changes in the hydrodynamic size of QDs [128]. First, CdTe–MPA QDs were prepared in aqueous solution phase. The thiol group of MPA is linked to the surface of CdTe QDs by thiol group-Cd coordination, and the functional carboxylic group is free, which can be easily coupled to biomolecules with amino groups, such as proteins, peptides, and amino acids. Coupling agent CDI, EDC, and EDC/sulfo-NHS were used to bioconjugate QDs with BSA. We studied the most suitable coupling agent for BSA conjugation with QDs. The CE was used for separation QD–BSA complex and unbounded QDs in the sample solution.

Figure 22 shows biomolecule conjugate electrophoretic behavior. The free QDs are well separated from QD–BSA within 10 min in the alkaline buffer (10 mM BBS). The migration times of conjugates were determined in comparison with non-conjugated QDs based upon their charge to-size ratio values. The QD–BSA conjugates were detected at a shorter migration time (2 min 40 s) compering free QDs (9 min 20 s) due to the inherent increase in the net negative charge of the conjugate. The isoelectric point (pI) of BSA is lower than CE buffer pH and thus increased number of negative charges that also influenced the net charge of the conjugate [32].

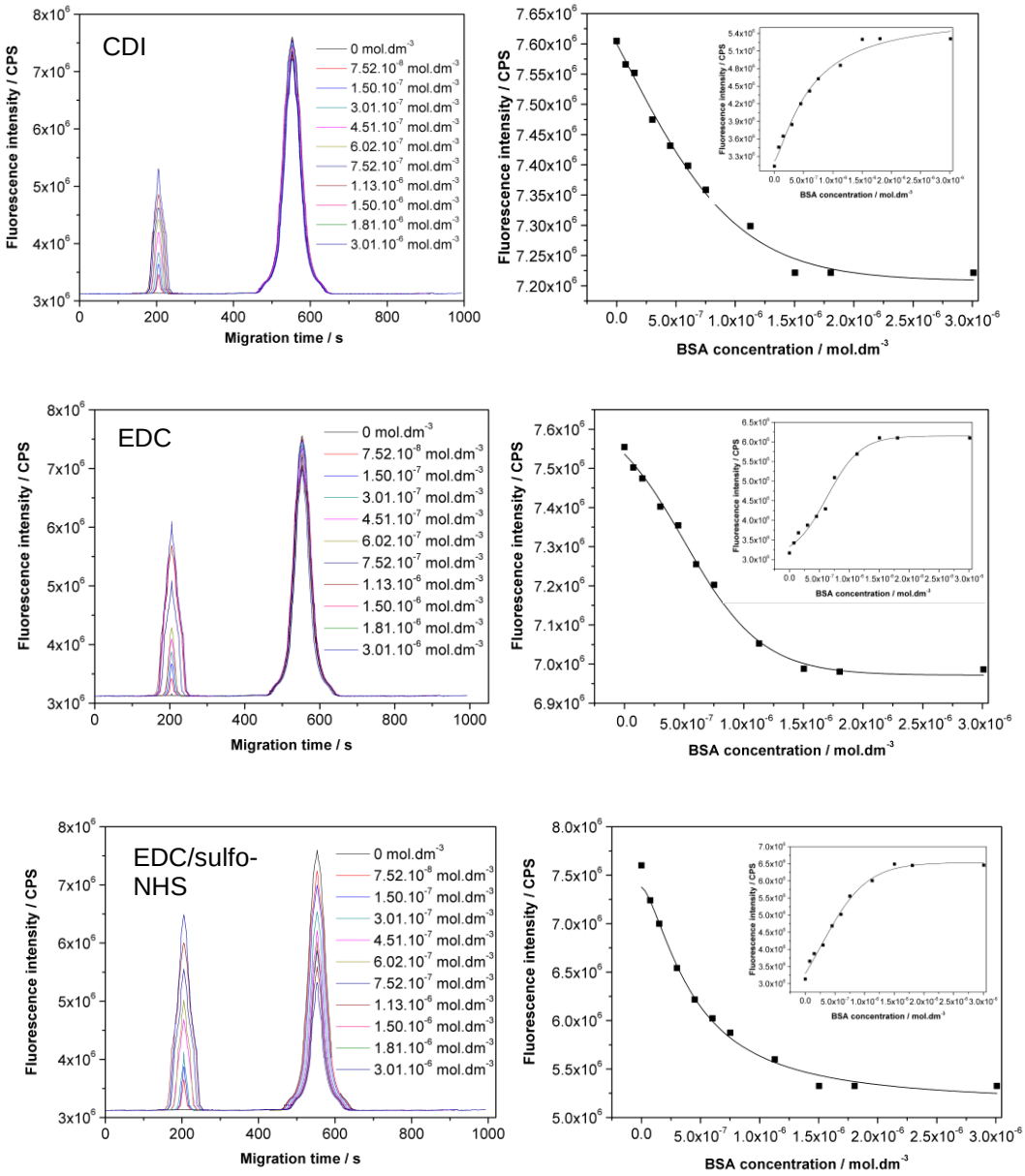


Figure 22 Electropherogram for separation of the CdTe-MPA QDs bioconjugated with various concentration of BSA, using different coupling agents, CDI, EDC and EDC/sulfo-NHS (left). Trend of QDs peak decreasing with increasing of BSA concentration was also shown (right). Inset: Trend of QDs-BSA peak increasing with increasing of BSA concentration. On a chip CE conditions- excitation: 380 nm; emission: 600 nm; channel: 50 µm, 10/4 cm; BGE: 10 mM Borate Buffered Saline (BBS), pH 9.4; voltage: 3 kV; electroosmotic flow (EOF) mobility $44.4 \cdot 10^{-9}$ $m^2 \cdot V^{-1} \cdot s^{-1}$.

The influence of increasing protein concentration on FL was studied. FL of free QDs (QDs peak) is decreasing and FL of QDs bioconjugates (QD–BSA peak) is increasing with increasing of protein concentration. In case of using CDI as a cross-linker, according to the plots (Figure 22, CDI right) at lower concentration of protein (in the range from 7.52 x $10^{-8}$

to 1.50 x $10^{-6}$ mol dm-3), QD peak intensity decreased for 5% (from 7.60 x $10^6$ CPS to 7.22 9 $10^6$ CPS) and QD– BSA peak intensity increased for 37% (from 3.13 x $10^6$ CPS to 5.29 x $10^6$ CPS) with a linear trend (Figure 22, CDI right inset). At higher concentration (>1.50 x $10^{-6}$ mol $dm^{-3}$) of protein, plateau on the dependence curve is noticed.

In case of using EDC as a cross-linker according to the plots (Figure 22, EDC right), at lower concentration of protein (in the range from 7.52 x $10^{-8}$ to 1.50 x $10^{-6}$ mol $dm^{-3}$), QD peak intensity decreased for 7.6% (from 7.55 x $10^6$ CPS to 6.98 x $10^6$ CPS) and QD–BSA peak intensity increased for 47% (from 3.16 x $10^6$ CPS to 6.01 x $10^6$ CPS) with a linear trend (Figure 22, EDC right inset). At higher concentration (>1.50 9 $10^{-6}$ mol $dm^{-3}$) of protein, plateau on the dependence curve is noticed. It was found that the addition of sulfo-NHS stabilizes the amine-reactive intermediate by converting it to a semi-stable amine-reactive sulfo-NHS ester, thereby increasing the efficiency of EDC mediated coupling reactions (Figure 12)[15].

In case of using EDC/sulfo-NHS as a cross-linker, according to the plots (Figure 22, EDC/sulfo-NHS right) at lower concentration (in the range from 7.52 x $10^{-8}$ to 7.25 x $10^{-7}$ mol $dm^{-3}$), QD peak intensity decreased for 30% (from 7.60 x $10^6$ CPS to 5.32 x $10^6$ CPS) and QD–BSA peak intensity increased for 52% (from 3.13 x $10^6$ CPS to 6.48 x $10^6$ CPS) with a linear trend (Figure 22, EDC/sulfo-NHS right inset). At higher concentration (< 1.13 x $10^{-6}$ mol $dm^{-3}$) of protein, plateau on the dependence curve is noticed. The most rapid decreasing and increasing of peaks intensity was noticed when using EDC/sulfo-NHS, compared to EDC and CDI. Plateau of peak shows a saturation of BSA ligands on a QD surface, and it occurs at 1.50 x $10^{-6}$ mol $dm^{-3}$ concentration of protein for CDI and EDC and at lower concentration of protein 7.25 x $10^{-7}$ mol $dm^{-3}$ for EDC/sulfo-NHS cross-linker. The sulfo-NHS ester is more effective at reacting with amine-containing molecules. When using this two-step process as opposed to using single-step EDC or CDI reaction, higher yields of amide bond formation may be achieved, which lead to saturation of BSA on QD surface at lower concentration.

## 5.2 Studying of fluorescence quenching of QDs caused by covalent conjugation with BSA

Quantum dots and BSA were conjugated via covalent coupling using three different agents CDI, EDC, and EDC/sulfo-NHS. FL intensity of bioconjugated QDs was measured by Tecan reader and it is decreasing with increasing of concentration of BSA. For further study of QD FL quenching, we processed different concentrations of protein up to 1.50 9 10-6 mol dm-3, where quenching effect is significant. Fluorescence-quenching effect of QDs caused by BSA can be described by the linear Stern–Volmer equation (6) [163].Where $I_0$ and I are steady-state FL intensities of QDs in the absence and presence of BSA, respectively, $K_{SV}$ is the Stern-Volmer quenching constant, and [Q] is the concentration of BSA. The $I_0/I$ were calculated according to (6) and plotted against BSA concentration (Figure 23).

The dependences exhibited very good linearity with coefficients of determination $R^2$ in

the range of 0.97–0.98 for all three coupling agents— CDI, EDC, and EDC/sulfoNHS. After linear fit, the slopes of the curves were calculated. The values represent $K_{SV}$ and the higher $K_{SV}$, the higher the quenching effect is [175]. The results show that the quenching constants vary for different types of bioconjugated QDs and depend on type of coupling agents used CDI, EDC, or EDC/sulfo-HNS and they are 3.64 x $10^4$, 5.59 x $10^4$,and 4.38 x $10^5$ $dm^3$ $mol^{-1}$,respectively,which is correspondent with values stated by other authors [176]. The Stern–Volmer plot of QD-quenching properties exhibited linear trend for the concentration given. This behavior suggests that only static quenching is taking place [177]. The results present that BSA can effectively quench FL of QDs in a ligand-dependent manner. In case where EDC/sulfo-NHS is used as a cross-linker, the FL is decreasing significantly, so the highest quenching effect was notable (see Figure 23).

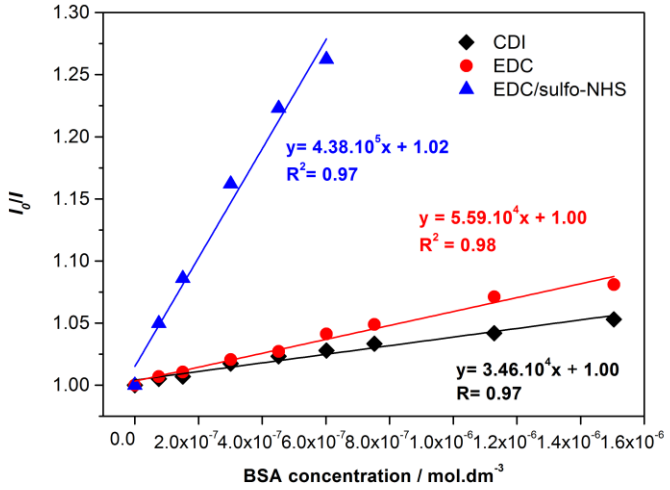


Figure 23 Stern–Volmer plots of BSA concentration dependence of FL intensity of QDs. $I_0$ and $I$are FL intensities of QDs in the absence and presence of BSA, respectively. Effect of cross-linker on a QD–BSA interaction was shown

The occurrence of static-quenching mechanism enlightened the presence of binding sites in the BSA. The binding sites and binding constant can be calculated from the following Equation (10) [176]:

$$\log\left[\frac{(I_0-I)}{I}\right] = \log K + n \cdot \log[Q] \qquad (10)$$

where K is the binding constant and n is number of binding sites between BSA and QDs. Based on (10) log [(I0-I)/I] were plotted against log[Q] for all three cross-linkers (Figure 24). The values of n (slope values) and K (intercept values) were calculated from the plots.

The results show that the binding constants vary for different types of bioconjugated QDs and depend on type of coupling agents used CDI, EDC, or EDC/sulfo-NHS and they are

$3.16 \times 10^3$, $9.18 \times 10^3$, and $2.24 \times 10^4$ $dm^3$ $mol^{-1}$, respectively. Values of binding constants calculated from this approach show similar trend as $K_{SV}$ calculated from the Stern–Volmer equation. The highest binding constant was determined for QDs coupled with BSA using EDC/sulfo-NHS. These results again confirm that the quenching mechanism is the static (complex formation) [176]. The number of binding sites is close to 1 for different ligands of QDs, suggesting that there is only one type of interaction between BSA and QDs [178].

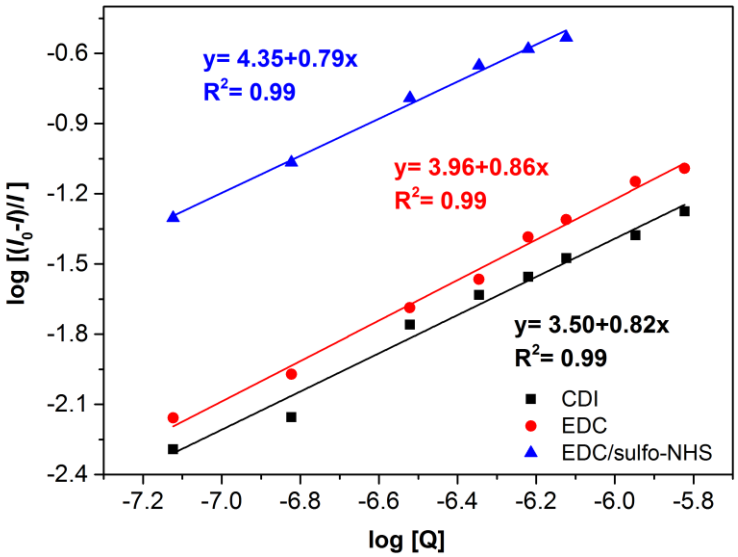


Figure 24 Plots of log $[(I_0 - I)/I]$ versus log[$Q$] for different cross-linkers. $I_0$ and $I$ are FL intensities of QDs in the absence and presence of BSA, respectively

The presence of BSA protein leads to strong quenching of FL emission, which could be explained by covalent interaction between the QDs and the quencher, demonstrating the formation of QD–BSA bioconjugates [40]. The sulfo-NHS ester is increasing the efficiency of coupling reactions; thus, the highest binding constant and quenching constant were determined when using EDC/sulfo-NHS as a cross-linker. The relative standard deviations of the migration time and peak area for QD–BSA with six runs were ≈2.1 and ≈8.7%, respectively.

# 6. ON A CHIP ELECTROPHORESIS IMMUNOASSAY FOR MULTIPLE ANTIBODIES

## 6.1 Electrophoretic analyses of antigen-antibody reaction products

The optimized system for efficient QD immunoassay based on a separation method should provide a clear resolution of three zones; the zone of unreacted QDs, free conjugates of QD with an antibody and the immunocomplex [19]. Such separation is demonstrated in Figure 25.

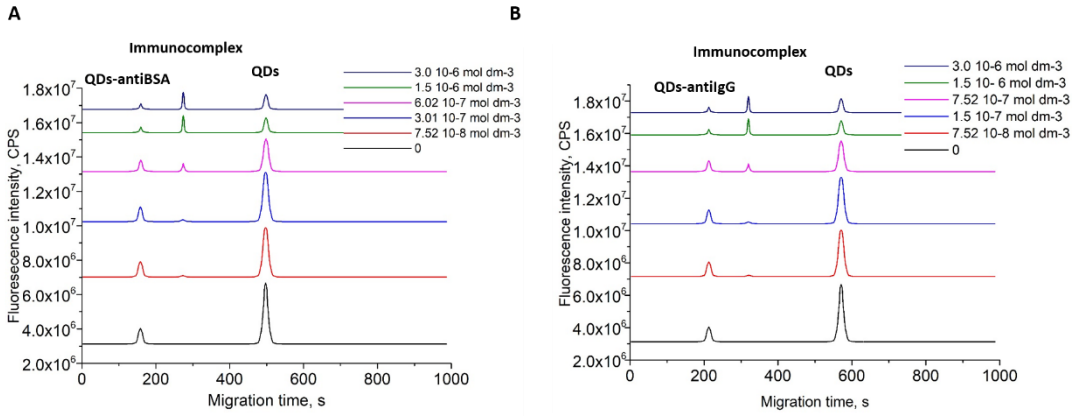


Figure 25 Electropherograms of separation of the Ab-QDs immunocomplexes with various concentrations of antigen. A) green QDs with BSA, B) Orange QDs with IgG

To evaluate analytic performance of the proposed strategy, the fluorescence intensity was measured in the presence of antigen at different concentrations. At lower concentrations of BSA (in the range from 0.005-0.1 mg/ml), QDs–Ab peak intensity decreased with a linear trend (Figure 26 A), while immunocomplex peak increased also with

a linear trend. At higher concentration of BSA (<0.1 mg/ml), a plateau on the dependence curve is noticed.

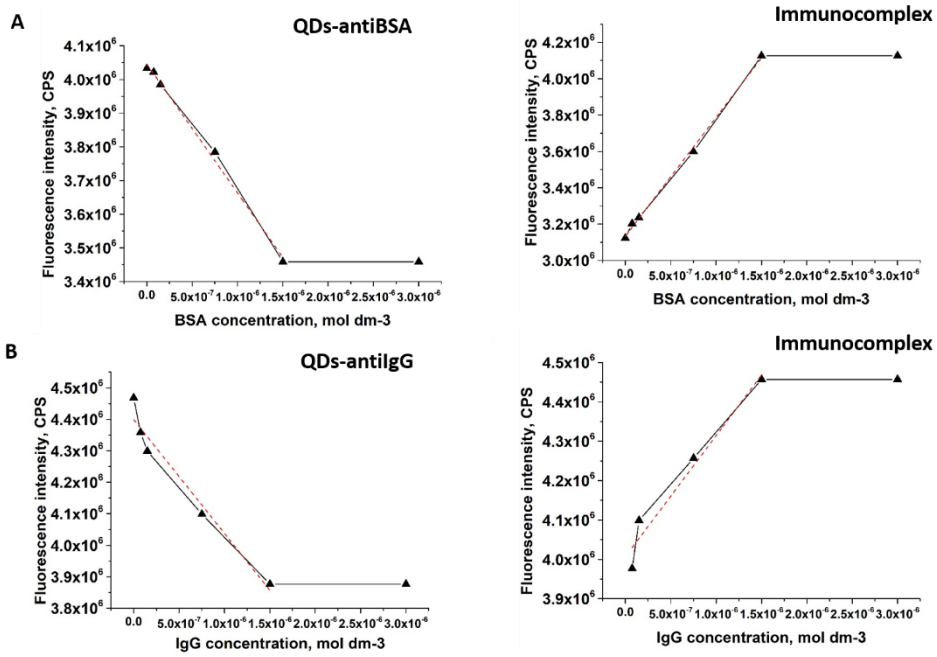


Figure 26 Dependence of QDs- antibody and immunocomplex peaks height on antigen concentration. A: Green QDs with BSA as an antigen, B: Orange QDs with IgG as an antigen

In case when IgG was used, same dependences for peaks are noticed. At the concentration of IgG in the range from 0.005-0.1 mg/ml, peak intensity of QDs–Ab peak intensity decreased with a linear trend (Figure 26), while immunocomplex peak increased also with a linear trend. At concentration of IgG above <0.1 mg/ml, plateau on the dependence curve is noticed again for all three peaks.

Reached plateau translates in a saturation of immunocomplex on a QD surface, and it occurs at 0.1 mg/mL concentration of antigen for both BSA and IgG. The decrease in QDs-Ab and increase in QDs immunocomplex peak height or area is proportional to the amount of BSA and IgG present. The linear curve fitted equation and coefficient of determination represented are listed in Table 3.

Table 3 The linear curve fitted equation and their coefficient of determination

| **Sample** | **Coefficient of determination,$R^2$** | **Regression equation** |
|---|---|---|
| Green QDs-BSA | 0.9956 | $y = -5.7 \times 10^6 x + 4.1 \times 10^6$ |
| Orange QDs-IgG | 0.9622 | $y = -5.4 \times 10^6 x + 4.4 \times 10^6$ |
| Green QDs- immunocomplex | 0.9981 | $y = 9.8 \times 10^6 x + 3.1 \times 10^6$ |
| Orange QDs- immunocomplex | 0.9566 | $y = 8.6 \times 10^6 x + 3.7 \times 10^6$ |

## 6.2 Comparison of CE immunoassay and solid-phase immunoassay techniques

Compared to conventional immunoassays, CE immunoassays offer several possible advantages. Two important advantages of CE immunoassays are their ease of automation and their relatively fast separation of antibodies, analytes and/or antibody-analyte complex [179]. In addition, CE immunoassays tend to consume only small amounts of sample and reagents while still allowing the detection of trace amounts of analyte in a sample[180]. The detection of multiple analytes in a single run is also feasible in a CE immunoassay, due to the high resolving power of modern capillary electrophoresis system [181]. Unfortunately, CE immunoassays tend to give poorer concentration-based limits of detection than solid-phase immunoassay techniques such as an enzyme-linked immunosorbent assay (ELISA) [182] .

Under these experimental conditions, limit of detection (LOD) of the immunocomplex was estimated to be 9.1 μg/mL for BSA detection and 5.4 μg/mL for mIgG. This LOD values are relatively higher than that obtained by conventional ELISA (ng/mL-pg/mL order). CE immunoassays tend to give poorer concentration-based LODs than solid-phase immunoassay technique such as ELISA [182]. This is a result of the analytes and antibodies both being present in solution in many CE immunoassay formats, while in ELISA a surface reaction can be used to pre-concentrate analytes for measurement and detection. Consequently, these results suggest that the proposed device would enable simple and rapid immunoassays with minimal amounts of samples and reagents.

These facts make difficult to apply our proposed device for immunoassays of extremely low-concentration targets such as tumor markers for cancer. On the other hand, for the analysis of high-concentration intravital samples such as human IgG (ca. 7-16 mg/mL), the proposed device would enable us to easily measure analytes with a shorter analysis time, in comparison to conventional ELISA methods. Consequently, these results suggest that the proposed device would enable simple and rapid immunoassays with minimal amounts of samples and reagents.

## 6.3 Electrophoretic separation of the antigen-antibody-QD complex (immunocomplex) from the free antigen and influence of QDs concentration

Influence of pure QDs peak area on a concentration of antigen was studied. Under these optimal experimental conditions, we noticed gradually decreasing of pure QDs peak, with the increase of antigen antibody concentration. Final concentration of QDs was 0.1 mg/ml (Figure 27).

At lower concentration of BSA (in the range from 0.005-0.1 mg/ml), pure QDs peak intensity decreased for 40.2% with a linear trend (Figure 27). At higher concentration of BSA (<0.1 mg/ml), plateau on the dependence curve is noticed (Figure 27, right inset).

In case when IgG was used, same dependence for peaks is noticed. At the concentration of IgG in the range from 0.005-0.1 mg/ml, pure QDs peak intensity decreased for 40.7% with a linear trend (Figure 27, B right inset). At concentration of IgG above <0.1 mg/ml, plateau on the dependence curve is noticed

The decrease in QDs and QDs-Ab and increase in QDs immunocomplex peak height or area is proportional to the amount of BSA and IgG present. The linear curve fitted equation and coefficient of determination represented are listed in Table 4.

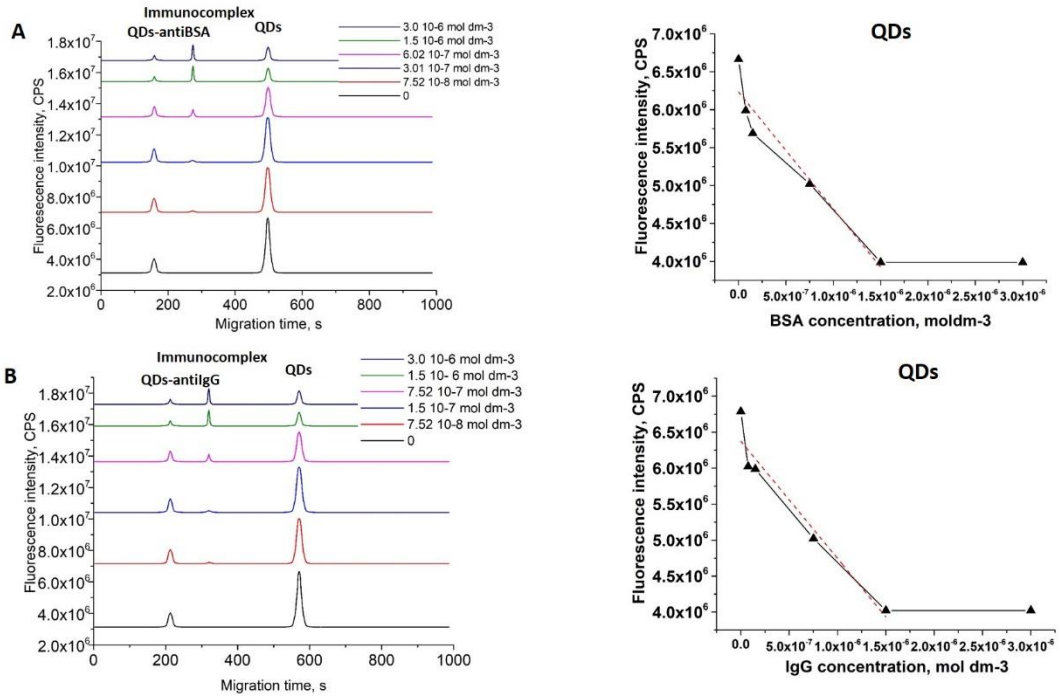


Figure 27 Electropherograms of separation of the Ab-QDs immunocomplexes with various concentrations of antigen. A) green QDs with BSA, B) Orange QDs with IgG (left). Dependence of QDs peak height on antigen concentration (right).

Table 4 The linear curve fitted equation and their coefficient of determination for pure QDs peak

| **Sample** | **Coefficient of determination,$R^2$** | **Regression equation** |
|---|---|---|
| Free green QDs | 0.9255 | $y = -2.3 \times 10^7 x + 6.2 \times 10^6$ |
| Free orange QDs | 0.9411 | $y = -2.4 \times 10^7 x + 6.4 \times 10^6$ |

Electrophoretic behavior of QD-biomolecule conjugate is shown in Figure 28. The free QDs are well separated from QDs- Ab and immunocomplex within 10 min in the alkaline buffer (10 mM BBS). The migration times of conjugates were determined in comparison with non-conjugated QDs based upon their charge to-size ratio values. Green QDs (1.8 nm ± 0.4) migrated faster towards detector than orange QDs (3.9 nm ± 0.7) due their smaller charge density. We were able to detect two different antigens simultaneously due its different size and charge. BSA as smaller protein migrated faster than IgG. The QD–BSA conjugates were detected at a shorter migration time (2 min 36 s) comparing to immunocomplex (4 min 31 s) and free green QDs (8 min 15 s). The QD-IgG conjugates were also detected at a shorter migration time (3 min 30 s) comparing to immunocomplex (5 min 17 s) and free orange QDs (9 min 28 s). Shorter migration time of conjugates and complex compare to free QDs occurs due to the inherent increase in the net negative charge of the conjugate. The isoelectric point (pI) of BSA (4.7) and IgG (7.0) is lower than CE buffer pH (8.2) and thus increased number of negative charges that also influenced the net charge of the conjugate [148].

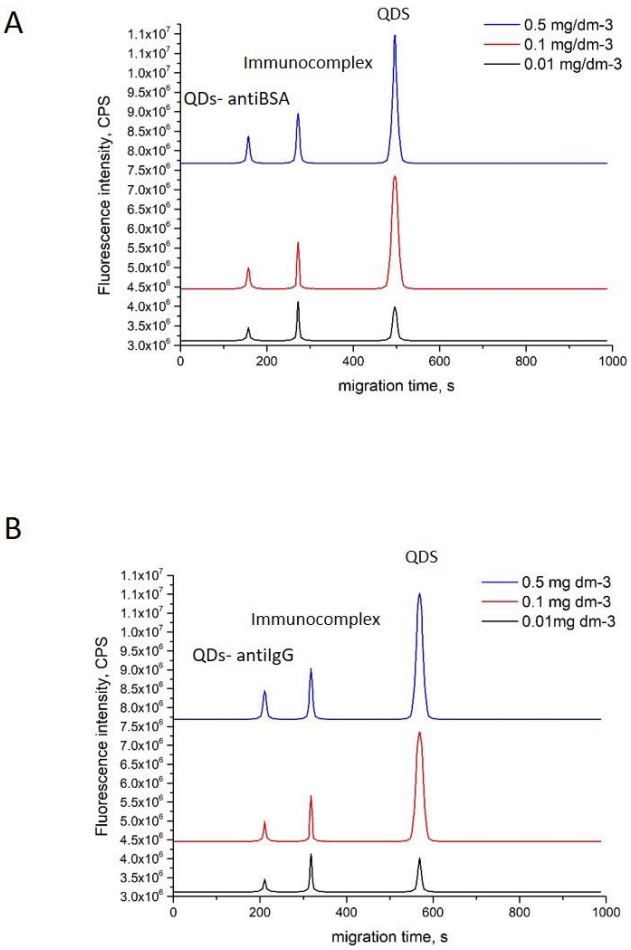


Figure 28 A: Electropherogram for separation of the CdTe–MPA QDs bioconjugated with A: green QDs with BSA, B: orange QDs with IgG, using different concentration of QDs (0.5, 0.1 and 0.01 mg/dm-3)

Figure 28 shows the complete separation of the conjugate and narrow peak of immunocomplex. It has already been described in literature that immunocomplex peak is much narrower than that of the QD-Ab conjugate [10]. This can be regarded as the evidence that only a limited number of the antibody molecules conjugated with QDs form a complex with the antigen. Thus, we can expect that the antibody conjugates capable of forming the immunocomplex are more homogeneous than those in the rest of the probe. Antibodies are complex structures with variable regions. The variation in the number of sialic acids attached to the heavy chain (Fc region) of an antibody causes the heterogeneity not only in its size but also in pI value. Another contribution to the polydispersity of a probe can be non-specific binding of the QDs at any primary amine group of a large antibody molecule. The antigen-binding sites of an antibody can even be blocked by attached QDs. All these facts can contribute significantly to the heterogeneity of the electrophoretic mobilites of immunoprobes, which negatively influence their separation resolution. In order to avoid this

problem we used monoclonal antibodies, which was earlier stated as a way to positively influence separation resolution [183].

In the next experiment, we studied how adding free CdTe QDs to solution will affect electrophoretic mobility and fluorescence intensity of QDs immunocomplex. Three different concentrations were used: 0.5, 0.1 and 0.01 mg/ml (Figure 28). Dependences of all three peaks on a QDs concentration is presented in Figure 29. We can clearly see that fluorescence intensity of free CdTe QDs peak increases progressively with increasing concentration of QDs. On the other hand, the adding of free QDs to a mixture after conjugation didn't provide any significant interaction of free QDs with conjugates and immunocomplex. There was no significant decreasing in peak area of QDs-Ab and immunocomplex peak with increasing of QDs concentration Figure 29. Same trend was stated by other authors [147].

In case when IgG was used, same dependence for peaks is noticed. The decrease in QDs and QDs-Ab and increase in QDs immunocomplex peak height or area is proportional to the amount of BSA and IgG present. The linear curve fitted equation and coefficient of determination represented are listed in Table 5.

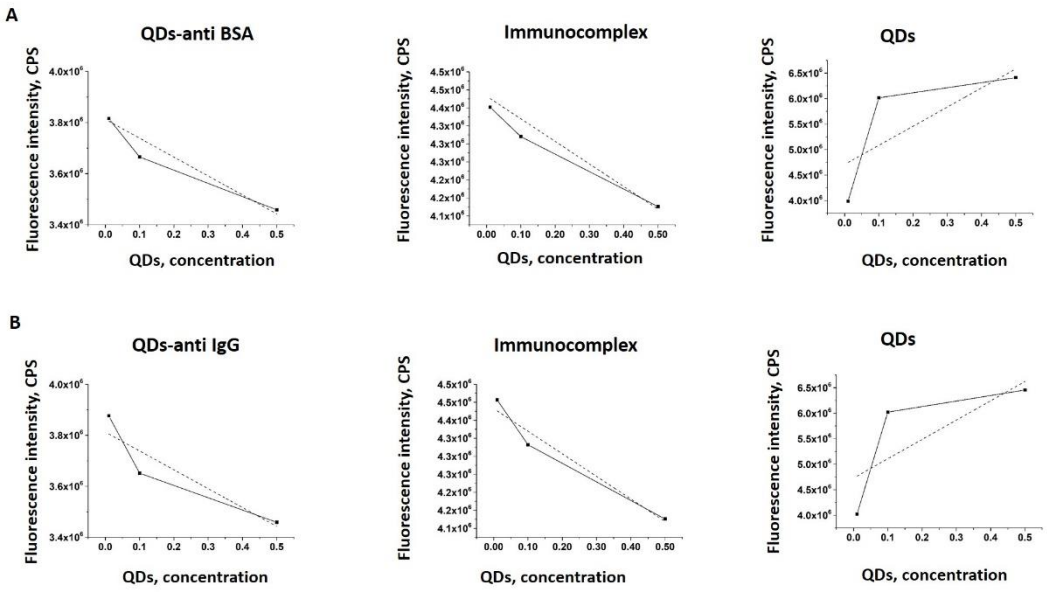


Figure 29 Dependence of pure QDs, QDs- antibody and immunocomplex peaks height on QDs concentration. A: Green QDs with BSA as an antigen, B: Orange QDs with IgG as an antigen.

Table 5 The linear curve fitted equation and their coefficient of determination

| Sample | Coefficient of determination,$R^2$ | Regression equation |
|---|---|---|
| Free green QDs | 0.7514 | $y = 3.7 \times 10^6 x + 4.7 \times 10^6$ |
| Free orange QDs | 0.7611 | $y = 3.8 \times 10^6 x + 4.6 \times 10^6$ |
| Green QDs-BSA | 0.7125 | $y = -7.3 \times 10^6 x + 3.9 \times 10^6$ |
| Orange QDs-IgG | 0.7042 | $y = -7.4 \times 10^6 x + 3.8 \times 10^6$ |
| Green QDs- immunocomplex | 0.9162 | $y = -6.2 \times 10^6 x + 4.5 \times 10^6$ |
| Orange QDs- immunocomplex | 0.9146 | $y = -6.3 \times 10^6 x + 4.4 \times 10^6$ |

## 6.4 Influence of the buffer to a separation in on a chip CE

In order to keep the migration velocity of weak electrolyte components and the velocity of the EOF constant, the regulation of the pH is an important purpose of the BGE. In that way a stable and reproducible migration behavior of the sample components can be obtained. The larger mobilities of substance, the faster their electrophoretic migration the shorter time of analysis. However, even substance with zero effective mobilities may move in the capillary due to the EOF and the EOF is strongly dependent of the pH of the BGE used.

Generally, the most powerful selectivity agent in CE is pH, and therefore it requires special consideration and control. Often, adequate selectivity can be obtained by simply adjusting the pH, and then the other separation conditions can be optimized for further purposes such as separation speed.

The concentration of the BGE can play an important part in the resolution of a separation in electrophoresis, dependent on several aspects. If a constant voltage is applied over the capillary, the electric current will increase for higher concentrations of the BGE and this can cause extra peak broadening due to a strong increase in the Joule heat. Further a higher concentration of the BGE gives a lower mobility of the EOF and by this, fast and medium fast anions cannot be determined in the cathodic mode. Often there is a strong attraction force between positively charged analytes and the negatively charged wall of the silica capillary resulting in broad tailing sample zones. A high concentration of the BGE can decrease this adhesive behavior of the sample ions by a competitive adsorption of the co-ions of the BGE, thus increasing the resolution. The counter ions of the BGE can show attraction forces with analytes and this complexation can be stronger at a high concentration of the BGE.

To overcome this additional heat care must be taken in choosing buffer type and concentration. After set of experiment used 10 mM BBS buffer (borate buffered saline, pH = 9. 14) was chosen for experiments in this study. Using 10 mM BBS buffer and 3kV voltage avoids overheating of PDMS walls and fluid.

In order to increase mobility of analytes we tried to increase the pH value of the

separation buffer. Usually, higher pH values would lead to similar increases in mobilities of both the immunocomplex and the antibody (Ab) hence could not improve the separation significantly. However, QD attached to the antibody could be a factor to influence the electrophoretic characteristics of the (Ab) and the complex in this study. The effect of QD on the Ab was greater than that on complex since both proteins, Ab and Ag, had contributions to the electrophoretic characteristics of the complex. Thus, the increase of buffer pH would amplify the effect of QD on the mobilities of the Ab and the complex. The mobility of the complex was expected to be influenced more by the buffer pH than that of the Ab peak.

The effects of buffer pH on the separation are shown in Figure 30. With the buffer of higher pH than 9.14, did not facilitate the formation of complex. The peak heights of the complex decreased at the pH 10.15 buffer and the peak of the complex disappeared eventually at pH 10.45. Optimal buffer pH value was set to 9.14 and the plate number.

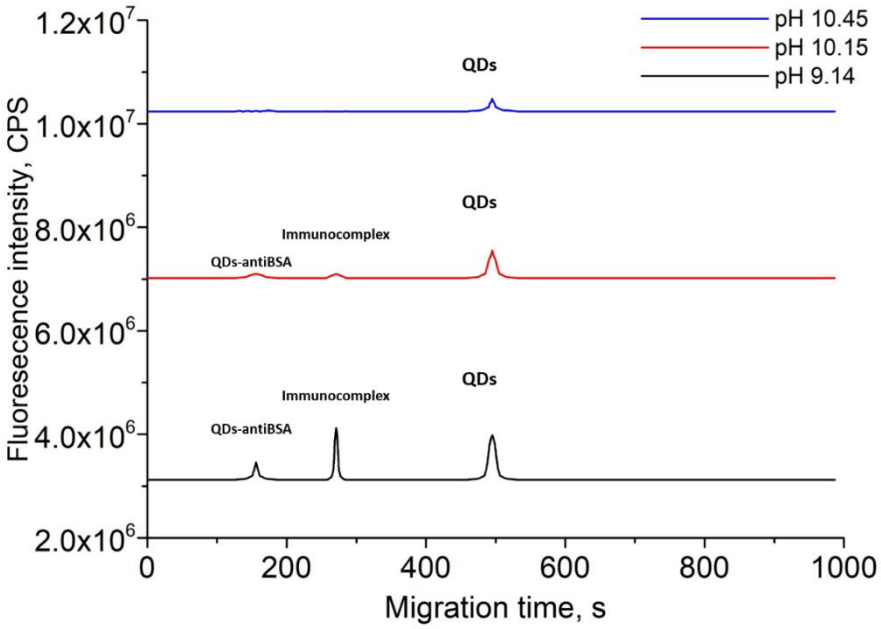


Figure 30 Effects of buffer pH values on a CdTe QDs antiBSA-BSA immunocomplex separation. Separation buffers: pH 9.14 (black), 10.15 (red) and 10.45 (blue).

## 6.5 CE on a chip immunoassay with both targets present

With the method presented in this chapter we were able to detect analytes conjugated with different size QDs at different emission wavelengths in a single run. Only one excitation light source was used and two filter systems for different emission wavelengths. In our portable experiment set up, filter, LED and detector can be easily removed and replaced by

other kind of equipment if needed for specific experiment. In Figure 31 electrophoretic behavior of a mixture of green QDs conjugated with immunocomplex BSA-anti BSA and orange QDs immunocomplex mIgG-anti mIgG run in experimental set up with two types of filter set up is presented.

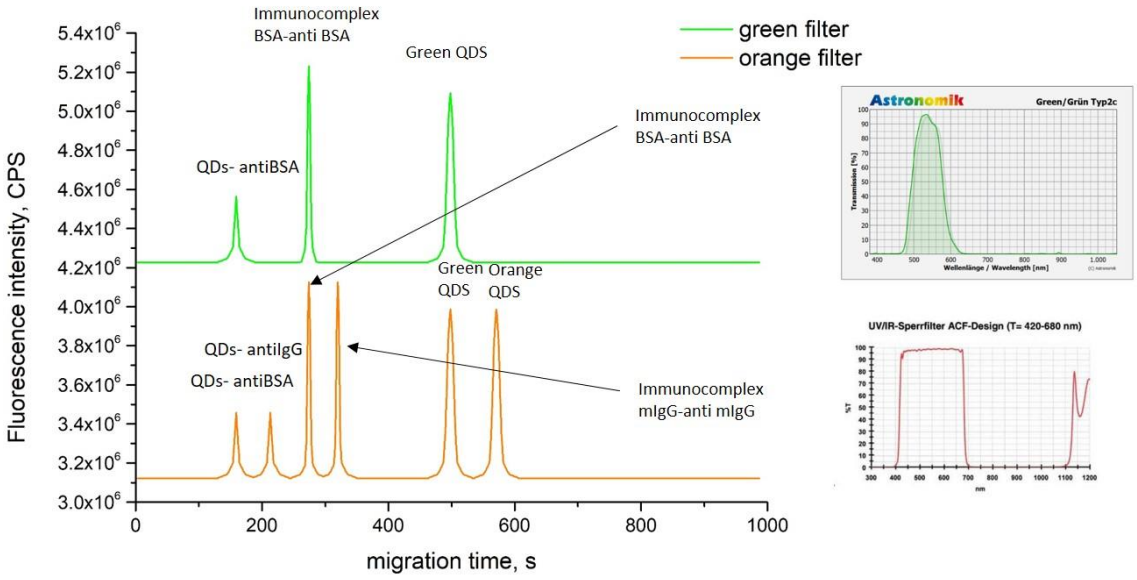


Figure 31 Electropherogram for separation of the mixture of two types of QDs 1. green CdTe–MPA QDs bioconjugated with BSA and 2. orange CdTe-MPA QDs bioconjugated with IgG. Using green and orange filter. Spectral characteristics of both filters are given on the left

The use of two filters with different wavelengths can distinguish the fluorescence coming from different size QDs. Using the 380 nm filter, fluorescence from orange QDs conjugates was completely filter out, as a result, only the fluorescence emission from green QDs and their conjugates is detected. Using the 420–680 nm high-pass optical filter, fluorescence from both orange and green QDs with their conjugates is detected. Using one excitation wavelength and two types of filter set up it was possible to detect two different immunocomplexes simultaneously.

# 7. CONCLUSION

QDs find a wide application in many different scientific filed, mostly in biology and medicine. Number of unique characteristic makes them especially interesting material for conjugation with biomolecules. Big issue in scientific world is toxicity of QDs. Due to increasing application of QDs in biology and medicine it is extremely important to better understand their interaction with biomolecules.

Biomodified QDs can be used in life science for drug delivery, luminescence tagging, implantable microdevices, and other. Further developing in this research field will depend on the understanding of specificity and capabilities of biomolecule–QD-coupling techniques and on the development of methods of characterization and separation of the conjugates. In this study, we successfully separated CdTe QDs bioconjugated with BSA using on-a-chip electrophoresis. Studying of quenching efficiency by measuring FL intensity showed that BSA is leading to a strong quenching effect of QD FL emission. Quenching effect depends on a coupling agent used to conjugate protein and it was the highest one when using EDC/sulfo-NHS.

In the work, we were able to get the quantitative detection of multiple antigen-antibody reaction on a single assay. Mixing two kinds of QDs bioconjugated with two different proteins and antibodies we were able to detect immunocomplex peaks with different areas which depends of concentration of QDs and antibody and antibody-antigen reaction. It is expected that CE immunoassays will continue to be explored for use in other clinical applications and to eventually mature into a method that is suitable for use in routine clinical laboratories.

The advantage of the work presented in this thesis is that it combines several improved techniques:

1. When using QDs instead of organic fluorophores a single light source can excite multicolor QDs without signal overlap
2. Using on a chip CE has its own advantages like simplicity, small sample and reagent requirements and high efficiency
3. When using portable experiment set up filter, LED and detector can be easily removed and replaced by other kind of equipment if needed for specific experiment.

Overall, the method developed can be applied to the determinations of other large bio-molecules in clinical and environmental applications. The adoption of this method should be further enhanced as advances continue to be made in the stability, precision and cost of CE systems for retinue chemical analysis.

# REFERENCES


1. Mattoussi, H., G. Palui, and H.B. Na, *Luminescent quantum dots as platforms for probing in vitro and in vivo biological processes.* Advanced Drug Delivery Reviews, 2012. **64**(2): p. 138-166.
2. Tomczak, N., et al., *Designer polymer-quantum dot architectures.* Progress in Polymer Science, 2009. **34**(5): p. 393-430.
3. Pinaud, F., et al., *Advances in fluorescence imaging with quantum dot bio-probes.* Biomaterials, 2006. **27**(9): p. 1679-1687.
4. Chomoucka, J., et al., *Cell toxicity and preparation of streptavidin-modified iron nanoparticles and glutathione-modified cadmium-based quantum dots.* Procedia Engineering, 2010. **5**: p. 922-925.
5. Hoshino, A., et al., *Physicochemical Properties and Cellular Toxicity of Nanocrystal Quantum Dots Depend on Their Surface Modification.* Nano Letters, 2004. **4**(11): p. 2163-2169.
6. Morelli, E., et al., *Chemical stability of CdSe quantum dots in seawater and their effects on a marine microalga.* Aquatic Toxicology, 2012. **122–123**(0): p. 153-162.
7. Huang, X., et al., *Characterization of quantum dot bioconjugates by capillary electrophoresis with laser-induced fluorescent detection.* Journal of Chromatography A, 2006. **1113**(1–2): p. 251-254.
8. Mamedova, N.N., et al., *Albumin-CdTe nanoparticle bioconjugates: Preparation, structure, and interunit energy transfer with antenna effect.* Nano Letters, 2001. **1**(6): p. 281-286.
9. Wang, J.H., et al., *Bioconjugation of concanavalin and CdTe quantum dots and the detection of glucose.* Colloids and Surfaces a-Physicochemical and Engineering Aspects, 2010. **364**(1-3): p. 82-86.
10. Feng, H.T., et al., *Immunoassay by capillary electrophoresis with quantum dots.* Journal of Chromatography A, 2007. **1156**(1-2): p. 75-79.
11. Goldman, E.R., et al., *Conjugation of Luminescent Quantum Dots with Antibodies Using an Engineered Adaptor Protein To Provide New Reagents for Fluoroimmunoassays.* Analytical Chemistry, 2002. **74**(4): p. 841-847.
12. Pathak, S., M.C. Davidson, and G.A. Silva, *Characterization of the Functional Binding Properties of Antibody Conjugated Quantum Dots.* Nano Letters, 2007. **7**(7): p. 1839-1845.
13. Ji, X., et al., *(CdSe)ZnS Quantum Dots and Organophosphorus Hydrolase Bioconjugate as Biosensors for Detection of Paraoxon.* The Journal of Physical Chemistry B, 2005. **109**(9): p. 3793-3799.
14. Dwarakanath, S., et al., *Quantum dot-antibody and aptamer conjugates shift fluorescence upon binding bacteria.* Biochemical and Biophysical Research Communications, 2004. **325**(3): p. 739-743.
15. Shan, Y., et al., *NHS-mediated QDs-peptide/protein conjugation and its application for cell labeling.* Talanta, 2008. **75**(4): p. 1008-1014.
16. Jimenez-López, J., et al., *Automated determination of Rifamycins making use of MPA–CdTe quantum dots.* Journal of Luminescence, 2016. **175**: p. 158-164.
17. Wang, J., et al., *Probing Antigen-Antibody Interaction Using Fluorescence Coupled Capillary Electrophoresis.* International Journal of Molecular Sciences, 2013. **14**(9): p. 19146.
18. Narain, R., *Chemistry of Bioconjugates: Synthesis, Characterization, and Biomedical Applications*. 2013, USA: Wiley. 496.
19. Pathak, S., et al., *Hydroxylated quantum dots as luminescent probes for in situ*

*hybridization.* Journal of the American Chemical Society, 2001. **123**(17): p. 4103-4104.
20. Song, X.T., et al., *Highly efficient size separation of CdTe quantum dots by capillary gel electrophoresis using polymer solution as sieving medium.* Electrophoresis, 2006. **27**(7): p. 1341-1346.
21. Nandi, P. and S.M. Lunte, *Recent trends in microdialysis sampling integrated with conventional and microanalytical systems for monitoring biological events: A review.* Analytica Chimica Acta, 2009. **651**(1): p. 1-14.
22. Amundsen, L.K. and H. Siren, *Immunoaffinity CE in clinical analysis of body fluids and tissues.* Electrophoresis, 2007. **28**(1-2): p. 99-113.
23. Liu, D., et al., *Current developments and applications of microfluidic technology toward clinical translation of nanomedicines.* Advanced Drug Delivery Reviews, 2018. **128**: p. 54-83.
24. Chiem, N.H. and D.J. Harrison, *Microchip systems for immunoassay: an integrated immunoreactor with electrophoretic separation for serum theophylline determination.* Clinical Chemistry, 1998. **44**(3): p. 591-598.
25. Chiem, N. and D.J. Harrison, *Microchip-based capillary electrophoresis for immunoassays: Analysis of monoclonal antibodies and theophylline.* Analytical Chemistry, 1997. **69**(3): p. 373-378.
26. Fister, J.C., et al., *Counting single chromophore molecules for ultrasensitive analysis and separations on microchip devices.* Analytical Chemistry, 1998. **70**(3): p. 431-437.
27. Moser, A.C., C.W. Willicott, and D.S. Hage, *Clinical applications of capillary electrophoresis based immunoassays.* Electrophoresis, 2014. **35**(7): p. 937-955.
28. Sang, F.M., X.Y. Huang, and J.C. Ren, *Characterization and separation of semiconductor quantum dots and their conjugates by capillary electrophoresis.* Electrophoresis, 2014. **35**(6): p. 793-803.
29. Maryatiy, M., et al., *A fluorescence-based assay suitable for quantitative analysis of deadenylase enzyme activity.* Nucleic Acids Research, 2014. **42**(5).
30. Swartzman, E.E., et al., *A homogeneous and multiplexed immunoassay for high-throughput screening using fluorometric microvolume assay technology.* Analytical Biochemistry, 1999. **271**(2): p. 143-151.
31. Becker, S., et al., *Ultra-high-throughput screening based on cell-surface display and fluorescence-activated cell sorting for the identification of novel biocatalysts.* Current Opinion in Biotechnology, 2004. **15**(4): p. 323-329.
32. Resch-Genger, U., et al., *Quantum dots versus organic dyes as fluorescent labels.* Nature Methods, 2008. **5**(9): p. 763-775.
33. Doria, G., et al., *Noble metal nanoparticles for biosensing applications.* Sensors (Basel, Switzerland), 2012. **12**(2): p. 1657-1687.
34. Rasooly, A. and K.E. Herold, *Analytical Methods | Biosensors*, in *Encyclopedia of Dairy Sciences (Second Edition)*, J.W. Fuquay, Editor. 2011, Academic Press: San Diego. p. 235-247.
35. Spindel, S. and K.E. Sapsford, *Evaluation of Optical Detection Platforms for Multiplexed Detection of Proteins and the Need for Point-of-Care Biosensors for Clinical Use.* Sensors, 2014. **14**(12): p. 22313-22341.
36. Gencoglu, A. and A.R. Minerick, *Electrochemical detection techniques in micro- and nanofluidic devices.* Microfluidics and Nanofluidics, 2014. **17**(5): p. 781-807.
37. Pan, Y.C., K. Karns, and A.E. Herr, *Microfluidic electrophoretic mobility shift assays for quantitative biochemical analysis.* Electrophoresis, 2014. **35**(15): p. 2078-2090.
38. Harrison, D.J., R.D. Oleschuk, and P. Thibault, *Microfluidic systems for analysis of the proteome with mass spectrometry*, in *Lab-on-a-Chip*, R.E. Oosterbroek and A.v.d. Berg, Editors. 2003, Elsevier: Amsterdam. p. 249-270.
39. Pires, N.M.M., et al., *Recent Developments in Optical Detection Technologies in Lab-on-a-Chip Devices for Biosensing Applications.* Sensors, 2014. **14**(8): p. 15458-15479.

40. Manz, A., et al., *PLANAR CHIPS TECHNOLOGY FOR MINIATURIZATION OF SEPARATION SYSTEMS - A DEVELOPING PERSPECTIVE IN CHEMICAL MONITORING.* Advances in Chromatography, 1993. **33**: p. 1-66.
41. Ceddia, M.G., et al., *A complex system perspective on the emergence and spread of infectious diseases: Integrating economic and ecological aspects.* Ecological Economics, 2013. **90**(0): p. 124-131.
42. Chin, C.D., V. Linder, and S.K. Sia, *Lab-on-a-chip devices for global health: Past studies and future opportunities.* Lab on a Chip, 2007. **7**(1): p. 41-57.
43. Kharsany, A.B.M. and Q.A. Karim, *HIV Infection and AIDS in Sub-Saharan Africa: Current Status, Challenges and Opportunities.* The Open AIDS Journal, 2016. **10**: p. 34-48.
44. Whitesides, G.M., *The origins and the future of microfluidics.* Nature, 2006. **442**(7101): p. 368-373.
45. Smith, J.P., et al., *Microfluidic transport in microdevices for rare cell capture.* Electrophoresis, 2012. **33**(21): p. 3133-3142.
46. Weibel, D.B. and G.M. Whitesides, *Applications of microfluidics in chemical biology.* Current Opinion in Chemical Biology, 2006. **10**(6): p. 584-591.
47. Schulte, T.H., R.L. Bardell, and B.H. Weigl, *Microfluidic technologies in clinical diagnostics.* Clinica Chimica Acta, 2002. **321**(1–2): p. 1-10.
48. Bayraktar, T. and S.B. Pidugu, *Characterization of liquid flows in microfluidic systems.* International Journal of Heat and Mass Transfer, 2006. **49**(5–6): p. 815-824.
49. Dhanasekaran, J. and D.L. Koch, *The hydrodynamic lift of a slender, neutrally buoyant fibre in a wall-bounded shear flow at small Reynolds number.* Journal of Fluid Mechanics, 2019. **879**: p. 121-146.
50. Koo, H.J. and O.D. Velev, *Ionic current devices-Recent progress in the merging of electronic, microfluidic, and biomimetic structures.* Biomicrofluidics, 2013. **7**(3).
51. Temiz, Y., et al., *A comparative study on fabrication techniques for on-chip microelectrodes.* Lab on a Chip, 2012. **12**(22): p. 4920-4928.
52. Misiakos, K., et al., *Fully integrated monolithic optoelectronic transducer for real-time protein and DNA detection: The NEMOSLAB approach.* Biosensors and Bioelectronics, 2010. **26**(4): p. 1528-1535.
53. Novo, P., V. Chu, and J.P. Conde, *Integrated optical detection of autonomous capillary microfluidic immunoassays:a hand-held point-of-care prototype.* Biosensors and Bioelectronics, 2014. **57**: p. 284-291.
54. Nie, Z., et al., *Integration of paper-based microfluidic devices with commercial electrochemical readers.* Lab on a Chip, 2010. **10**(22): p. 3163-3169.
55. Balasubramanian, V., et al., *A 0.18$\mu {\rm m}$Biosensor Front-End Based on$1/f$Noise, Distortion Cancelation and Chopper Stabilization Techniques.* IEEE Transactions on Biomedical Circuits and Systems, 2013. **7**(5): p. 660-673.
56. Saylor, R.A. and S.M. Lunte, *A review of microdialysis coupled to microchip electrophoresis for monitoring biological events.* Journal of Chromatography A, 2015. **1382**: p. 48-64.
57. Le, H.P., *Progress and trends in ink-jet printing technology.* Journal of Imaging Science and Technology, 1998. **42**(1): p. 49-62.
58. Terry, S.C., *A gas chromatography system fabricated on a silicon wafer using integrated circuit technology*. 1975, UMI: Ann Arbor, Mich.
59. Manz, A., N. Graber, and H.M. Widmer, *Miniaturized total chemical analysis systems: A novel concept for chemical sensing.* Sensors and Actuators B: Chemical, 1990. **1**(1): p. 244-248.
60. Harrison, D.J., et al., *Capillary electrophoresis and sample injection systems integrated on a planar glass chip.* Analytical Chemistry, 1992. **64**(17): p. 1926-1932.
61. Apple, F.S., et al., *Simultaneous Rapid Measurement of Whole Blood Myoglobin, Creatine Kinase MB, and Cardiac Troponin I by the Triage Cardiac Panel for Detection of*

*Myocardial Infarction.* Clinical Chemistry, 1999. **45**(2): p. 199-205.
62. Nguyen, H.V., et al., *Nucleic acid diagnostics on the total integrated lab-on-a-disc for point-of-care testing.* Biosensors & Bioelectronics, 2019. **141**: p. 8.
63. Kwon, S. and S.J. Choi, *Development of Tubing-based Stationary Liquid-phase Enzyme-linked Immunosorbent Assay.* Biochip Journal, 2019. **13**(2): p. 174-181.
64. Zhu, C.C., et al., *A Lab-on-a-Chip Device Integrated DNA Extraction and Solid Phase PCR Array for the Genotyping of High-Risk HPV in Clinical Samples.* Micromachines, 2019. **10**(8): p. 12.
65. Park, B. and S.J. Choi, *Sensitive immunoassay-based detection of Vibrio parahaemolyticus using capture and labeling particles in a stationary liquid phase lab-on-a-chip.* Biosensors & Bioelectronics, 2017. **90**: p. 269-275.
66. Wang, J., et al., *A paper-based device with an adjustable time controller for the rapid determination of tumor biomarkers.* Sensors and Actuators B-Chemical, 2018. **254**: p. 855-862.
67. Jacobson, S.C., et al., *High-Speed Separations on a Microchip.* Analytical Chemistry, 1994. **66**(7): p. 1114-1118.
68. Wu, D., J. Qin, and B. Lin, *Electrophoretic separations on microfluidic chips.* Journal of Chromatography A, 2008. **1184**(1–2): p. 542-559.
69. Culbertson, C.T., et al., *Micro Total Analysis Systems: Fundamental Advances and Biological Applications.* Analytical Chemistry, 2014. **86**(1): p. 95-118.
70. Wang, Y., Q. Lin, and T. Mukherjee, *A model for Joule heating-induced dispersion in microchip electrophoresis.* Lab on a Chip, 2004. **4**(6): p. 625-631.
71. Zhao, C.L., et al., *Electrokinetically driven continuous-flow enrichment of colloidal particles by Joule heating induced temperature gradient focusing in a convergent-divergent microfluidic structure.* Scientific Reports, 2017. **7**: p. 12.
72. Xuan, X. and D. Li, *Analytical study of Joule heating effects on electrokinetic transportation in capillary electrophoresis.* Journal of Chromatography A, 2005. **1064**(2): p. 227-237.
73. Jones, A.E. and E. Grushka, *Nature of temperature gradients in capillary zone electrophoresis.* Journal of Chromatography A, 1989. **466**: p. 219-225.
74. Ghosal, S., *Fluid mechanics of electroosmotic flow and its effect on band broadening in capillary electrophoresis.* Electrophoresis, 2004. **25**(2): p. 214-228.
75. Qi, C. and C.O. Ng, *Electroosmotic flow of a power-law fluid through an asymmetrical slit microchannel with gradually varying wall shape and wall potential.* Colloids and Surfaces a-Physicochemical and Engineering Aspects, 2015. **472**: p. 26-37.
76. Good, N.E., et al., *Hydrogen Ion Buffers for Biological Research*.* Biochemistry, 1966. **5**(2): p. 467-477.
77. Boček, P., P. Gebauer, and J.L. Beckers, *Success and failure with phthalate buffers in capillary zone electrophoresis.* ELECTROPHORESIS, 2001. **22**(6): p. 1106-1111.
78. Erickson, D., D. Sinton, and D.Q. Li, *Joule heating and heat transfer in poly(dimethylsiloxane) microfluidic systems.* Lab on a Chip, 2003. **3**(3): p. 141-149.
79. Davies, C., *Chapter 1.3 - Immunoassay Performance Measures11This chapter is from the first edition of The Immunoassay Handbook, with few changes, because of the high regard in which Chris Davies' original material is held. The theory still applies but some of the examples given are dated*, in *The Immunoassay Handbook (Fourth Edition)*, D. Wild, Editor. 2013, Elsevier: Oxford. p. 11-26.
80. Darwish, I.A., *Immunoassay Methods and their Applications in Pharmaceutical Analysis: Basic Methodology and Recent Advances.* International journal of biomedical science : IJBS, 2006. **2**(3): p. 217-235.
81. Moser, A.C. and D.S. Hage, *Capillary electrophoresis-based immunoassays: Principles and quantitative applications.* Electrophoresis, 2008. **29**(16): p. 3279-3295.
82. Miki, S., T. Kaneta, and T. Imasaka, *Immunoassay for human serum albumin using*

*capillary electrophoresis-semiconductor laser-induced fluorometry.* Journal of Chromatography B, 2001. **759**(2): p. 337-342.
83. Sheehan, C., J. He, and M. Smith, *Chapter 5.2 - Method Evaluation—A Practical Guide*, in *The Immunoassay Handbook (Fourth Edition)*, D. Wild, Editor. 2013, Elsevier: Oxford. p. 395-402.
84. Durner, J., *Clinical Chemistry: Challenges for Analytical Chemistry and the Nanosciences from Medicine.* Angewandte Chemie-International Edition, 2010. **49**(6): p. 1026-1051.
85. He, Z.H., N. Gao, and W.R. Jin, *Capillary electrophoretic enzyme immunoassay with electrochemical detection using a noncompetitive format.* Journal of Chromatography B-Analytical Technologies in the Biomedical and Life Sciences, 2003. **784**(2): p. 343-350.
86. Schmerr, M.J., et al., *Use of capillary electrophoresis and fluorescent labeled peptides to detect the abnormal prion protein in the blood of animals that are infected with a transmissible spongiform encephalopathy.* Journal of Chromatography A, 1999. **853**(1-2): p. 207-214.
87. Glazer, A.N. and C.S. Hixson, *SUBUNIT STRUCTURE AND CHROMOPHORE COMPOSITION OF RHODOPHYTAN PHYCOERYTHRINS - PORPHYRIDIUM-CRUENTUM B-PHYCOERYTHRIN AND B-PHYCOERYTHRIN.* Journal of Biological Chemistry, 1977. **252**(1): p. 32-42.
88. Kim, H., D.-R. Chung, and M. Kang, *A new point-of-care test for the diagnosis of infectious diseases based on multiplex lateral flow immunoassays.* Analyst, 2019. **144**(8): p. 2460-2466.
89. McDonnell, B., et al., *Cardiac biomarkers and the case for point-of-care testing.* Clinical Biochemistry, 2009. **42**(7): p. 549-561.
90. Jaffe, A.S., L. Babuin, and F.S. Apple, *Biomarkers in Acute Cardiac Disease: The Present and the Future.* Journal of the American College of Cardiology, 2006. **48**(1): p. 1-11.
91. Quinn, D.A., et al., *D-dimers in the diagnosis of pulmonary embolism.* American Journal of Respiratory and Critical Care Medicine, 1999. **159**(5): p. 1445-1449.
92. Yager, P., G.J. Domingo, and J. Gerdes, *Point-of-Care Diagnostics for Global Health.* Annual Review of Biomedical Engineering, 2008. **10**(1): p. 107-144.
93. Dohnalová, K., et al., *Surface brightens up Si quantum dots: direct bandgap-like size-tunable emission.* Light: Science &Amp; Applications, 2013. **2**: p. e47.
94. Chan, W.C.W. and S. Nie, *Quantum Dot Bioconjugates for Ultrasensitive Nonisotopic Detection.* Science, 1998. **281**(5385): p. 2016-2018.
95. Hu, J., et al., *Linearly Polarized Emission from Colloidal Semiconductor Quantum Rods.* Science, 2001. **292**(5524): p. 2060-2063.
96. Efros, A.L., *Luminescence polarization of CdSe microcrystals.* Physical Review B, 1992. **46**(12): p. 7448-7458.
97. Empedocles, S.A., R. Neuhauser, and M.G. Bawendi, *Three-dimensional orientation measurements of symmetric single chromophores using polarization microscopy.* Nature, 1999. **399**: p. 126.
98. Rasmussen, T.E., et al., *Single Molecule Applications of Quantum Dots.* Journal of Modern Physics, 2013. **Vol.04No.11**: p. 16.
99. Dabbousi, B.O., et al., *(CdSe)ZnS Core–Shell Quantum Dots: Synthesis and Characterization of a Size Series of Highly Luminescent Nanocrystallites.* The Journal of Physical Chemistry B, 1997. **101**(46): p. 9463-9475.
100. Ozkan, M., *Quantum dots and other nanoparticles: what can they offer to drug discovery?* Drug Discovery Today, 2004. **9**(24): p. 1065-1071.
101. Lakowicz, J.R., *Principles of fluorescence spectroscopy*. 1999: Second edition. New York : Kluwer Academic/Plenum, [1999] ©1999.
102. van de Weert, M., *Fluorescence Quenching to Study Protein-ligand Binding: Common Errors.* Journal of Fluorescence, 2010. **20**(2): p. 625-629.
103. Murray, C.B., D.J. Norris, and M.G. Bawendi, *Synthesis and characterization of nearly monodisperse CdE (E = sulfur, selenium, tellurium) semiconductor nanocrystallites.*

Journal of the American Chemical Society, 1993. **115**(19): p. 8706-8715.
104. Medintz, I.L., et al., *Quantum dot bioconjugates for imaging, labelling and sensing.* Nature Materials, 2005. **4**: p. 435.
105. Sergey, B.B. and F.R. Vladimir, *Colloidal quantum dots: synthesis, properties and applications.* Russian Chemical Reviews, 2016. **85**(12): p. 1297.
106. Hakkarainen, T., et al., *Chapter 12 - Site-Controlled Epitaxy of InAs Quantum Dots on Nanoimprint Lithography Patterns*, in *Molecular Beam Epitaxy (Second Edition)*, M. Henini, Editor. 2018, Elsevier. p. 277-292.
107. Mattoussi, H., G. Palui, and H.B. Na, *Luminescent Quantum Dots as Platforms for Probing in Vitro and in Vivo Biological Processes.* Advanced Drug Delivery Reviews, 2011(0).
108. Carrillo-Carrión, C., B.M. Simonet, and M. Valcárcel, *Determination of amines based on their interaction with QDs: Effect of the formation QD-assemblies.* Analytica Chimica Acta, 2011. **703**(2): p. 212-218.
109. Wan, Z., W. Luan, and S.-t. Tu, *Continuous synthesis of CdSexTe1−x nanocrystals: Chemical composition gradient and single-step capping.* Journal of Colloid and Interface Science, 2011. **356**(1): p. 78-85.
110. Kjällman, T., et al., *Quenching of an indocarbocyanine dye and functionalized CdSe/ZnS quantum dots by gold surfaces.* Current Applied Physics, 2008. **8**(3-4): p. 308-311.
111. Liu, X., et al., *Synthesis and spectrum stability of high quality CdTe quantum dots capped with stearate groups in N-oleoylmorpholine solvent.* Journal of Crystal Growth, 2010. **312**(19): p. 2656-2660.
112. Li, Z., et al., *Preparation and characterization of CdS quantum dots chitosan biocomposite.* Reactive and Functional Polymers, 2003. **55**(1): p. 35-43.
113. Majumder, M., S. Karan, and B. Mallik, *Study of steady state and time resolved photoluminescence of thiol capped CdS nanocrystalline powders dispersed in N,N-dimethylformamide.* Journal of Luminescence, 2011. **131**(12): p. 2792-2802.
114. Bae, P.K., et al., *The modification of quantum dot probes used for the targeted imaging of his-tagged fusion proteins.* Biomaterials, 2009. **30**(5): p. 836-842.
115. Mekis, I., et al., *One-pot synthesis of highly luminescent CdSe/CdS core-shell nanocrystals via organometallic and "greener" chemical approaches.* Journal of Physical Chemistry B, 2003. **107**(30): p. 7454-7462.
116. Zheng, Y.G., S.J. Gao, and J.Y. Ying, *Synthesis and cell-imaging applications of glutathione-capped CdTe quantum dots.* Advanced Materials, 2007. **19**(3): p. 376-+.
117. He, Y., et al., *Microwave-assisted growth and characterization of water-dispersed CdTe/CdS core-shell nanocrystals with high photoluminescence.* Journal of Physical Chemistry B, 2006. **110**(27): p. 13370-13374.
118. Zhang, H., et al., *The influence of carboxyl groups on the photoluminescence of mercaptocarboxylic acid-stabilized CdTe nanoparticles.* Journal of Physical Chemistry B, 2003. **107**(1): p. 8-13.
119. Liu, Y.-F. and J.-S. Yu, *Selective synthesis of CdTe and high luminescence CdTe/CdS quantum dots: The effect of ligands.* Journal of Colloid and Interface Science, 2009. **333**(2): p. 690-698.
120. Xu, W.B., et al., *Optimized synthesis and fluorescence spectrum analysis of CdSe quantum dots.* Journal of Dispersion Science and Technology, 2008. **29**(7): p. 953-957.
121. Abd El-sadek, M.S., et al., *Influence of different stabilizers on the optical and nonlinear optical properties of CdTe nanoparticles.* Optics Communications, 2011. **284**(12): p. 2900-2904.
122. Cui, R., et al., *Versatile immunosensor using CdTe quantum dots as electrochemical and fluorescent labels.* Analytical Chemistry, 2007. **79**(22): p. 8494-8501.
123. Algar, W.R. and U.J. Krull, *Characterization of the adsorption of oligonucleotides on mercaptopropionic acid-coated CdSe/ZnS quantum dots using fluorescence resonance energy transfer.* Journal of Colloid and Interface Science, 2011. **359**(1): p. 148-154.

124. Aldeek, F., et al., *The influence of capping thioalkyl acid on the growth and photoluminescence efficiency of CdTe and CdSe quantum dots.* Nanotechnology, 2008. **19**(47).
125. Huang, C.-P., Y.-K. Li, and T.-M. Chen, *A highly sensitive system for urea detection by using CdSe/ZnS core-shell quantum dots.* Biosensors and Bioelectronics, 2007. **22**(8): p. 1835-1838.
126. Saran, A.D., et al., *An optimized quantum dot-ligand system for biosensing applications: Evaluation as a glucose biosensor.* Colloids and Surfaces A: Physicochemical and Engineering Aspects, 2011. **384**(1-3): p. 393-400.
127. Yuan, J., et al., *Glutathione-capped CdTe quantum dots for the sensitive detection of glucose.* Talanta, 2009. **77**(5): p. 1858-1863.
128. Vicente, G. and L.A. Colon, *Separation of bioconjugated quantum dots using capillary electrophoresis.* Analytical Chemistry, 2008. **80**(6): p. 1988-1994.
129. Bruchez Jr, M., et al., *Semiconductor nanocrystals as fluorescent biological labels.* Science, 1998. **281**(5385): p. 2013-2016.
130. Yang, H., et al., *A Novel Quantum Dots–Based Point of Care Test for Syphilis.* Nanoscale Research Letters, 2010. **5**(5): p. 875.
131. Wu, X., et al., *Immunofluorescent labeling of cancer marker Her2 and other cellular targets with semiconductor quantum dots.* Nature Biotechnology, 2002. **21**: p. 41.
132. Sapsford, K.E., et al., *Functionalizing Nanoparticles with Biological Molecules: Developing Chemistries that Facilitate Nanotechnology.* Chemical Reviews, 2013. **113**(3): p. 1904-2074.
133. Bilan, R., et al., *Quantum Dot Surface Chemistry and Functionalization for Cell Targeting and Imaging.* Bioconjugate Chemistry, 2015. **26**(4): p. 609-624.
134. Blanco-Canosa, J.B., et al., *Recent progress in the bioconjugation of quantum dots.* Coordination Chemistry Reviews, 2014. **263-264**: p. 101-137.
135. Foubert, A., et al., *Bioconjugation of quantum dots: Review & impact on future application.* TrAC Trends in Analytical Chemistry, 2016. **83**: p. 31-48.
136. Palui, G., et al., *Strategies for interfacing inorganic nanocrystals with biological systems based on polymer-coating.* Chemical Society Reviews, 2015. **44**(1): p. 193-227.
137. Steinitz, M., *Quantitation of the Blocking Effect of Tween 20 and Bovine Serum Albumin in ELISA Microwells.* Analytical Biochemistry, 2000. **282**(2): p. 232-238.
138. Wedege, E. and G. Svenneby, *Effects of the blocking agents bovine serum albumin and Tween 20 in different buffers on immunoblotting of brain proteins and marker proteins.* Journal of Immunological Methods, 1986. **88**(2): p. 233-237.
139. Steinbusch, H.W.M., A.A.J. Verhofstad, and H.W.J. Joosten, *Localization of serotonin in the central nervous system by immunohistochemistry: Description of a specific and sensitive technique and some applications.* Neuroscience, 1978. **3**(9): p. 811-819.
140. Hu, Y.-J., et al., *Studies of interaction between colchicine and bovine serum albumin by fluorescence quenching method.* Journal of Molecular Structure, 2005. **750**(1): p. 174-178.
141. Painter, R.H., *IgG*, in *Encyclopedia of Immunology (Second Edition)*, P.J. Delves, Editor. 1998, Elsevier: Oxford. p. 1208-1211.
142. *Chapter 9 - Antibodies*, in *Immunology for Pharmacy*, D.K. Flaherty, Editor. 2012, Mosby: Saint Louis. p. 70-78.
143. So, M.-K., et al., *Self-illuminating quantum dot conjugates for in vivo imaging.* Nature Biotechnology, 2006. **24**: p. 339.
144. Didenko, V.V., H. Ngo, and D.S. Baskin, *Polyethyleneimine as a transmembrane carrier of fluorescently labeled proteins and antibodies.* Analytical Biochemistry, 2005. **344**(2): p. 168-173.
145. Parak, W.J., et al., *Conjugation of DNA to silanized colloidal semiconductor nanocrystalline quantum dots.* Chemistry of Materials, 2002. **14**(5): p. 2113-2119.

146. Nehilla, B.J., T.Q. Vu, and T.A. Desai, *Stoichiometry-dependent formation of quantum dot-antibody bioconjugates: A complementary atomic force microscopy and agarose gel electrophoresis study.* Journal of Physical Chemistry B, 2005. **109**(44): p. 20724-20730.
147. Kleparnik, K., et al., *Capillary electrophoresis immunoassays with conjugated quantum dots.* Electrophoresis, 2011. **32**(10): p. 1217-1223.
148. Pereira, M. and E.P. Lai, *Capillary electrophoresis for the characterization of quantum dots after non-selective or selective bioconjugation with antibodies for immunoassay.* Journal of Nanobiotechnology, 2008. **6**(1): p. 10.
149. Lafont, F., et al., *DNA-dependent protein kinase activity assessed by quantum dot-based microarray.* Febs Journal, 2017. **284**: p. 113-113.
150. Geho, D., et al., *Pegylated, steptavidin-conjugated quantum dots are effective detection elements for reverse-phase protein microarrays.* Bioconjugate Chemistry, 2005. **16**(3): p. 559-566.
151. Delehanty, J.B., et al., *Active cellular sensing with quantum dots: Transitioning from research tool to reality; a review.* Analytica Chimica Acta, 2012. **750**(0): p. 63-81.
152. Speranskaya, E.S., et al., *Hydrophilic, Bright CuInS2 Quantum Dots as Cd-Free Fluorescent Labels in Quantitative Immunoassay.* Langmuir, 2014. **30**(25): p. 7567-7575.
153. Taranova, N.A., et al., *'Traffic light' immunochromatographic test based on multicolor quantum dots for the simultaneous detection of several antibiotics in milk.* Biosensors and Bioelectronics, 2015. **63**: p. 255-261.
154. Kim, M.J., et al., *Western blot analysis using metal–nitrilotriacetate conjugated CdSe/ZnS quantum dots.* Analytical Biochemistry, 2008. **379**(1): p. 124-126.
155. Xu, W., et al., *A homogeneous immunosensor for AFB1 detection based on FRET between different-sized quantum dots.* Biosensors and Bioelectronics, 2014. **56**: p. 144-150.
156. Shamirian, A., A. Ghai, and P. Snee, *QD-Based FRET Probes at a Glance.* Sensors, 2015. **15**(6): p. 13028.
157. Sapsford, K., et al., *Biosensing with Luminescent Semiconductor Quantum Dots.* Sensors, 2006. **6**(8): p. 925.
158. Clarke, S., et al., *Covalent Monofunctionalization of Peptide-Coated Quantum Dots for Single-Molecule Assays.* Nano Letters, 2010. **10**(6): p. 2147-2154.
159. Medintz, I.L., et al., *Self-assembled nanoscale biosensors based on quantum dot FRET donors.* Nature Materials, 2003. **2**: p. 630.
160. Bailey, R.E., A.M. Smith, and S. Nie, *Quantum dots in biology and medicine.* Physica E: Low-dimensional Systems and Nanostructures, 2004. **25**(1): p. 1-12.
161. Long, Z., et al., *Visual enantioselective probe based on metal organic framework incorporating quantum dots.* Microchemical Journal, 2013. **110**: p. 764-769.
162. Liskova, M., et al., *Conjugation reactions in the preparations of quantum dot-based immunoluminescent probes for analysis of proteins by capillary electrophoresis.* Analytical and Bioanalytical Chemistry, 2011. **400**(2): p. 369-379.
163. Tian, J.N., et al., *Controllable synthesis and cell-imaging studies on CdTe quantum dots together capped by glutathione and thioglycolic acid.* Journal of Colloid and Interface Science, 2009. **336**(2): p. 504-509.
164. Chopra, A., et al., *CdTe nanobioprobe based optoelectrochemical immunodetection of diabetic marker HbA1c.* Biosensors & Bioelectronics, 2013. **44**: p. 132-135.
165. Bubendorfer, A.J., et al., *Contamination of PDMS microchannels by lithographic molds.* Lab on a Chip, 2013. **13**(22): p. 4312-4316.
166. Roman, G.T., K. McDaniel, and C.T. Culbertson, *High efficiency micellar electrokinetic chromatography of hydrophobic analytes on poly( dimethylsiloxane) microchips.* Analyst, 2006. **131**(2): p. 194-201.
167. Thorslund, S. and F. Nikolajeff, *Instant oxidation of closed microchannels.* Journal of Micromechanics and Microengineering, 2007. **17**(4): p. N16-N21.
168. Filla, L.A., D.C. Kirkpatrick, and R.S. Martin, *Use of a Corona Discharge to Selectively*

*Pattern a Hydrophilic/Hydrophobic Interface for Integrating Segmented Flow with Microchip Electrophoresis and Electrochemical Detection.* Analytical Chemistry, 2011. **83**(15): p. 5996-6003.
169. Vickers, J.A., M.M. Caulum, and C.S. Henry, *Generation of Hydrophilic Poly(dimethylsiloxane) for High-Performance Microchip Electrophoresis.* Analytical Chemistry, 2006. **78**(21): p. 7446-7452.
170. McDonald, J.C., et al., *Fabrication of microfluidic systems in poly(dimethylsiloxane).* Electrophoresis, 2000. **21**(1): p. 27-40.
171. Zhou, J.W., A.V. Ellis, and N.H. Voelcker, *Recent developments in PDMS surface modification for microfluidic devices.* Electrophoresis, 2010. **31**(1): p. 2-16.
172. Jai Kumar, B., D. Sumanth Kumar, and H.M. Mahesh, *A facile single injection Hydrothermal method for the synthesis of thiol capped CdTe Quantum dots as light harvesters.* Journal of Luminescence, 2016. **178**: p. 362-367.
173. Kimura, K., S. Takashima, and H. Ohshima, *Molecular Approach to the Surface Potential Estimate of Thiolate-Modified Gold Nanoparticles.* The Journal of Physical Chemistry B, 2002. **106**(29): p. 7260-7266.
174. Voráčová, I., et al., *Determination of ζ-potential, charge, and number of organic ligands on the surface of water soluble quantum dots by capillary electrophoresis.* ELECTROPHORESIS, 2015. **36**(6): p. 867-874.
175. Ryvolova, M., et al., *Glutathione modified CdTe quantum dots as a label for studying DNA interactions with platinum based cytostatics.* ELECTROPHORESIS, 2013. **34**(6): p. 801-808.
176. Vaishanav, S.K., et al., *Adsorption Kinetics and Binding Studies of Protein Quantum Dots Interaction: A Spectroscopic Approach.* Journal of Fluorescence, 2016. **26**(3): p. 855-865.
177. Ghali, M., *Static quenching of bovine serum albumin conjugated with small size CdS nanocrystalline quantum dots.* Journal of Luminescence, 2010. **130**(7): p. 1254-1257.
178. Ellappan, V., et al., *Interaction of digestive enzymes with tunable light emitting quantum dots: a thorough Spectroscopic investigation.* Luminescence, 2015. **30**(7): p. 978-989.
179. German, I. and R.T. Kennedy, *Rapid simultaneous determination of glucagon and insulin by capillary electrophoresis immunoassays.* Journal of Chromatography B, 2000. **742**(2): p. 353-362.
180. Phillips, T.M. and E.F. Wellner, *Analysis of inflammatory biomarkers from tissue biopsies by chip-based immunoaffinity CE.* Electrophoresis, 2007. **28**(17): p. 3041-3048.
181. Caslavska, J., D. Allemann, and W. Thormann, *Analysis of urinary drugs of abuse by a multianalyte capillary electrophoretic immunoassay.* Journal of Chromatography A, 1999. **838**(1-2): p. 197-211.
182. Heegaard, N.H.H. and R.T. Kennedy, *Identification, quantitation, and characterization of biomolecules by capillary electrophoretic analysis of binding interactions.* Electrophoresis, 1999. **20**(15-16): p. 3122-3133.
183. Shimura, K. and B.L. Karger, *Affinity probe capillary electrophoresis: analysis of recombinant human growth hormone with a fluorescent labeled antibody fragment.* Analytical Chemistry, 1994. **66**(1): p. 9-15.

# LIST OF FIGURES

# LIST OF TABLES

# LIST OF ACRONYMS

The following abbreviations are used in the text:

| | |
|---|---|
| BGE | background electrolyte |
| BSA | bovine serum albumin |
| CDI | Carbonyldiimidazole |
| CE | capillary electrophoresis |
| CE-LIF | laser-induced fluorescence detection |
| DLS | dynamic light-scattering |
| EDC | 1-ethyl-3-(3-dimethylaminopropyl)carbodiimide |
| ELISA | enzyme-linked immunosorbent assay |
| EOF | electroosmotic flow |
| FL | fluorescence |
| IC | integrated circuit |
| mIgG | mouse immunoglobulin G |
| LOC | Lab on a chip |
| NHS | N-hydroxysulfosuccinimide |
| NPs | Nanoparticles |
| PDMS | Polydimethylsiloxane |
| POC | point of care |
| PSA | prostate specific antigen |
| QDs | quantum dots |
| XRD | X-ray diffraction |

The following symbols are used in the text:

| | |
|---|---|
| $\mu$ | dynamic viscosity of fluid ($kg \cdot m^{-1} \cdot s^{-1}$) |
| P | density of the fluid ($kg\ m^{-3}$) |
| *D* | diameter of channel (m) |
| $d_{hydr}$ | Hydrodynamic diameter (m) |
| *v* | velocity of the analyte ($m\ s^{-1}$) |

| | |
|---|---|
| $\mu_e$ | electrophoretic mobility ($m^2\ v^{-1}\ s^{-1}$) |
| E | Electric field strength ($V\ m^{-1}$) |
| $q$ | charge of the ionized analyte (C) |
| $R$ | Radius (m) |
| $I_0$ | fluorescence intensities observed in the absence of quencher |
| $I$ | fluorescence intensities observed in the presence of quencher |
| $K_{Sv}$ | Stern-Volmer quenching constant. |
| $k_q$ | bimolecular quenching constant |
| $\tau_0$ | lifetime of the fluorophore in the absence of quencher. |

# AUTHORS PUBLICATIONS AND OTHER INPUTS

**PUBLICATIONS:**

PEJOVIČ SIMEUNOVIČ, J.; PEKÁRKOVÁ, J.; ŽÁK, J.; CHAMRADOVÁ, I.; HUBÁLEK, J. Studying of quantum dot luminescence quenching effect caused by covalent conjugation with protein. Monatshefte für Chemie, 2017, roč. 148, č. 11, s. 1901-1909. ISSN: 1434-4475.

KURZHALS, S.; SÜSS, M.; PEJOVIČ SIMEUNOVIČ, J.; VAN OOSTRUM, P.; REIMHULT, E.; ZIRBS, R. Crosslinking of floating colloidal monolayers. *Monatshefte für Chemie,* 2017, roč. 148, č. 8, s. 1539-1546. ISSN: 1434-4475.

SIMEUNOVIĆ, J. P.; GADJANSKI, I.; JANIĆIJEVIĆ, Ž.; JANKOVIĆ, M. M; BARJAKTAROVIĆ, M. M; JANKOVIĆ, N. Z; ČANTRAK Đ. S. Microfluidic Chip Fabrication for Application in Low-Cost DIY MicroPIV. In Proceedings of 5th International Conference on Advanced Manufacturing Engineering and Technologies. 1. Springer, Cham, 2017. s. 451-459. ISBN: 978-3-319-56430-2.

PEJOVIC SIMEUNOVIC, J.; HUBÁLEK, J. Separation and detection of bioconjugated quantum dots using on a chip electrophoresis. In Proceedings of the 22nd Conference STUDENT EEICT 2016. první. Brno: Vysoké učení technické v Brně, Fakulta elektrotechniky a komunikačních, 2016. s. 660-664. ISBN: 978-80-214-5350- 0.

PEJOVIC SIMEUNOVIC, J.; PEKÁRKOVÁ, J.; ŽAK, J.; HUBÁLEK, J. ON-A- CHIP ELECTROPHORESIS FOR THE CHARACTERIZATION OF QUANTUM DOTS BIOCONJUGATES. In CECE 2016, the 13 th International Interdisciplinary Meeting on Bioanalysis. Brno: Institute of Analytical Chemistry of the CAS, 2016. s. 211-214. ISBN: 978-80-904959-4-4.

PEJOVIC SIMEUNOVIC, J.; PEKÁRKOVÁ, J.; HUBÁLEK, J. Separation and detection of bioconjugated QDs in microfluidic devices using capillary electrophoresis. CEITEC PhD Retreat. 1. Brno: Masarykova univerzita, 2015. s. 109-109. ISBN: 978-80-210-7825- 3.

**PRODUCTS:**

ŽÁK, J.; SEDLÁČEK, J.; PEJOVIC, J.; PEKÁRKOVÁ, J.: HVElektroforezniZdroj; VN zdroj pro řízení kapilární elektroforézy. Technická 10, 0.66. URL: http://www.umel.feec.vutbr.cz/LabSensNano/products.aspx?id=91. (funkční vzorek)

**PROJECTS:**

GA16-11140S, Microfluidics-based Ultra Fast Differential Scaning Fluorometry for Drug Discovery (uDSF) start: 01.01.2016, end: 31.3.2017- research team member

Advanced nanotechnologies and materials, start: 01.01.2014, end: 31.12.2016

**FOREIGN INTERNSHIP:**

Doctoral internship (10.11.2014 - 19.12.2014. and 01.02.2015-31.07.2015.) at Universität für Bodenkultur Wien (BOKU), in Department of Nanobiotechnology (DNBT)